TOWER CSP
TECHNOLOGY
STATE OF THE ART AND
MARKET OVERVIEW

PROJETO **Energia**
Heliotérmica

PROJETO Energia Heliotérmica

A study produced by the project DKTI-CSP (German Climate Technology Initiative on Concentrating Solar Power), which is managed by the Ministry of Science, Technology and Innovation (MCTI) and the Gesellschaft für Internationale Zusammenarbeit (GIZ) GmbH. The project focusses on the promotion of climate technologies, in particular Concentrating Solar Power. Its objective is to ensure that required conditions to implement and disseminate Concentrating Solar Power are established in Brazil.

cooperação alemã
DEUTSCHE ZUSAMMENARBEIT

Implemented by:
giz
Deutsche Gesellschaft
für Internationale
Zusammenarbeit (GIZ) GmbH

Ministério da
**Ciência, Tecnologia
e Inovação**

GOVERNO FEDERAL
BRASIL
PÁTRIA EDUCADORA

TOWER CSP TECHNOLOGY
STATE OF THE ART AND
MARKET OVERVIEW

DLR

CONTENT

EXECUTIVE SUMMARY

A solar tower (or central receiver) system is a focus point solar thermal power plant. It consists of the following main components:

- **Heliostat field**: A large number of heliostats with flat or slightly curved mirror facets, tracked in two axes, to reflect the solar radiation onto the receiver
- **Receiver**: Absorbs the concentrated solar power and transfers the energy to a heat transfer medium
- **Tower**: Concrete or steel tower carrying the receiver on top
- **Storage**: Thermal storage system that enables electricity generation when no or insufficient solar power is available
- **Power block**: Power cycle converting thermal power to electricity

Solar tower systems differ from other solar power systems in the following aspects:

- The **concentration factor** is higher, in the range of 500 to 1000
- **Higher receiver temperatures** can be achieved with high efficiency
- Potential for higher annual **solar-to-electric efficiency** of 15 to 18% (up to 30% in design point conditions)
- Cost-effective thermal **storage** due to high temperature spread

While Parabolic trough is the most mature concentrating solar power technology in the market, solar tower technology is in an early phase of market introduction. However, solar tower systems offer a high cost reduction potential, according to many studies. This is already reflected in the increasing market share of solar towers for plants that were recently commissioned, are under construction or are announced. By the end of 2013 a total solar tower capacity of 104MW was online, corresponding to 3% of the total CSP capacity. The Ivanpah plant with 377MW was commissioned in February 2014, and further plants with a capacity of 210MW are under construction and will be completed in 2014.

The current status of the technology is discussed in detail, with emphasis on the technology that is used in today's commercial solar tower plants. Two solar tower technologies are in operation in commercial power plants:

a) systems that use a **direct steam** generating receiver that feeds a steam cycle, with no or **only limited storage capacity** installed and

b) systems that use **molten salt** as heat transfer and storage medium, with **high storage capacities**.

Such a molten salt system in Spain has already demonstrated successful commercial operation since April 2011. It has also proven **continuous operation for 36 days**. Actual annual solar-to-electric efficiencies are in the range of 15%.

There exist currently only a few companies worldwide that are offering solar tower plants. An overview on these companies is given in chapter 9, including basic economic figures and reference plants.

The LCOE of solar tower systems depends strongly on the system configuration and the annual direct normal insolation at the selected site. For typical solar tower plants **actual LCOE are in the range of 0.15 to 0.20€/kWh**. In the future, with increasing solar tower capacity installed, significant cost reductions are expected. Studies predict a **potential cost reduction down to less than 0.08€/kWh** (e.g. [67]).

Cost reductions are expected from technological innovations and cost reductions from mass production of components. New heliostat designs are under development, and innovative receiver concepts are proposed for higher process temperatures. Evolutionary changes will be implemented in the next generation of solar tower systems, but most of the innovative concepts still require significant development before entering the market.

Certain regions in Brazil have promising solar resources for CSP applications. Solar tower systems offer new markets for local suppliers. The range of components is from concrete structures over standard technical equipment to high precision and high reliability components, with a significant potential for manufacturing in Brazil. The specific requirements of solar tower system components are discussed in the Appendix.

1 INTRODUCTION

1.1 CONCENTRATING SOLAR POWER

Concentrating solar power (often also named "Solar Thermal Electricity", STE) technology uses optical concentrators to create high solar flux levels on so-called receivers. In the receiver the solar radiation is absorbed and converted to heat. The heat is transferred to a heat transfer medium which is transported to a thermal power cycle (or a storage system for later use). In the power cycle the heat is converted to electricity that is fed to the grid.

Among all renewable power systems, the main advantages of CSP plants are:
• Generation of dispatchable power (due to integrated thermal storage)
• Ensured grid capacity (due to optional co-firing)

Because of these unique features, CSP plants are considered as an important factor in the future energy mix with high shares of renewables.

CSP technology experienced a first boom after the first oil crisis in the last century. During the years 1984 until 1990 the first commercial solar power plants were built in the USA, with a total capacity of 354MW. These plants were maintained regularly and are still in operation. Then, in a period of low energy prices, no new CSP plants were built due to economic reasons. With increasing energy prices and the evidence of global warming from greenhouse gas emissions the implementation of renewable energy systems into the power market became more important. Around the year 2007 the installation of new CSP plants started, supported by political and legislative support (e. g. "Renewable Portfolio Standard" in the US, "Feed-in Tariff" in Spain). Since then, the total installed capacity of CSP plants has significantly grown (Fig. 1).

GLOBAL CUMULATIVE INSTALLED CSP CAPACITY
MW, 2007-2012
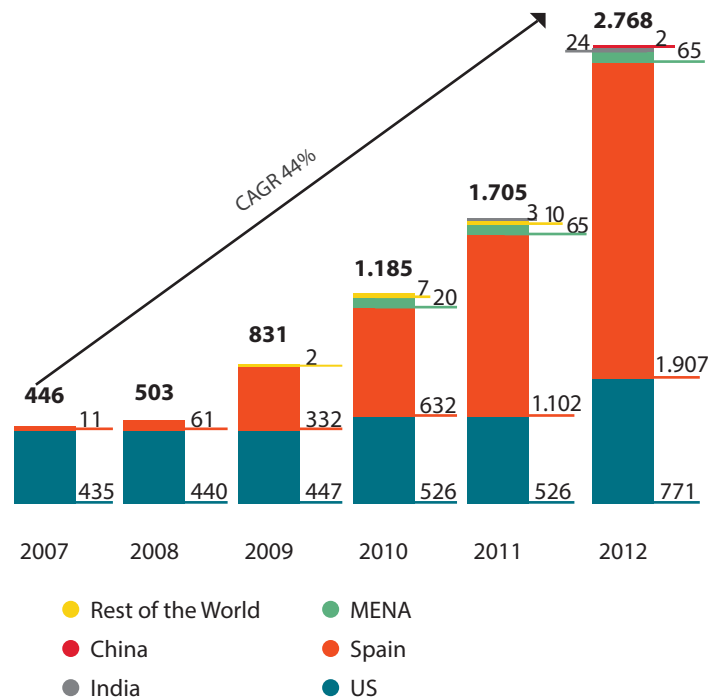
Figure 1: Cumulative CSP capacity worldwide [4]

In 2013, the total cumulative CSP capacity reached 3438MW worldwide [2]. The majority of this amount was built as Parabolic trough plants (3280MW or 95.4%). Solar tower systems contributed with 104MW (3%), followed by Linear Fresnel systems with 53MW (1.5%). Dish-Stirling systems had a negligible share.

A major requirement for CSP is the availability of high direct solar radiation levels (i. e. clear sky conditions), as concentrating solar systems can only convert the direct solar radiation into power. Diffuse radiation (cloudy sky) cannot be concentrated and is therefore not usable in a CSP system. Generally, an annual direct normal insolation (DNI) level of 2000kWh/m²a (~5.5kWh/m²/day) is considered as the minimum level for the economic feasibility of CSP plants. However, the economic viability might differ significantly with DNI, region, legislation, local power system etc.

Figure 2: Solar resource map of Brazil (DNI) [1]

The solar DNI resource of Brazil is shown in Fig. 2. According to the mentioned minimum radiation level the region from north of Belo Horizonte up to Fortaleza seems to offer suitable conditions for CSP plants.

There are currently four CSP technologies available that differ mainly in the method of concentration of the solar radiation. Two concentrator families exist:

- Linear focus: Solar radiation is concentrated to a focal line, with typical concentration levels up to 100
- Point focus: Solar radiation is concentrated to a focal point, with typical concentration levels up to 1000

Another characteristic is the receiver integration, with the options "moving receiver" and "fixed receiver". Using the above characteristics, the four CSP technologies can be categorized as shown in Table 1.

Table 1: Categories of CSP systems

Characteristic	Fixed receiver	Moving receiver
Line focus	Linear Fresnel	Parabolic trough
Point focus	Solar tower	Parabolic dish

Schematics of the different CSP technologies are depicted in Fig. 3.

Parabolic trough

Reflector

Absorber tube

Solar field piping

Central receiver

Solar Tower

Heliostats

Linear Fresnel reflector (IFR)

Curved mirrors

Absorber tube and reconcentrator

Parabolic dish

Receiver/engine

Reflector
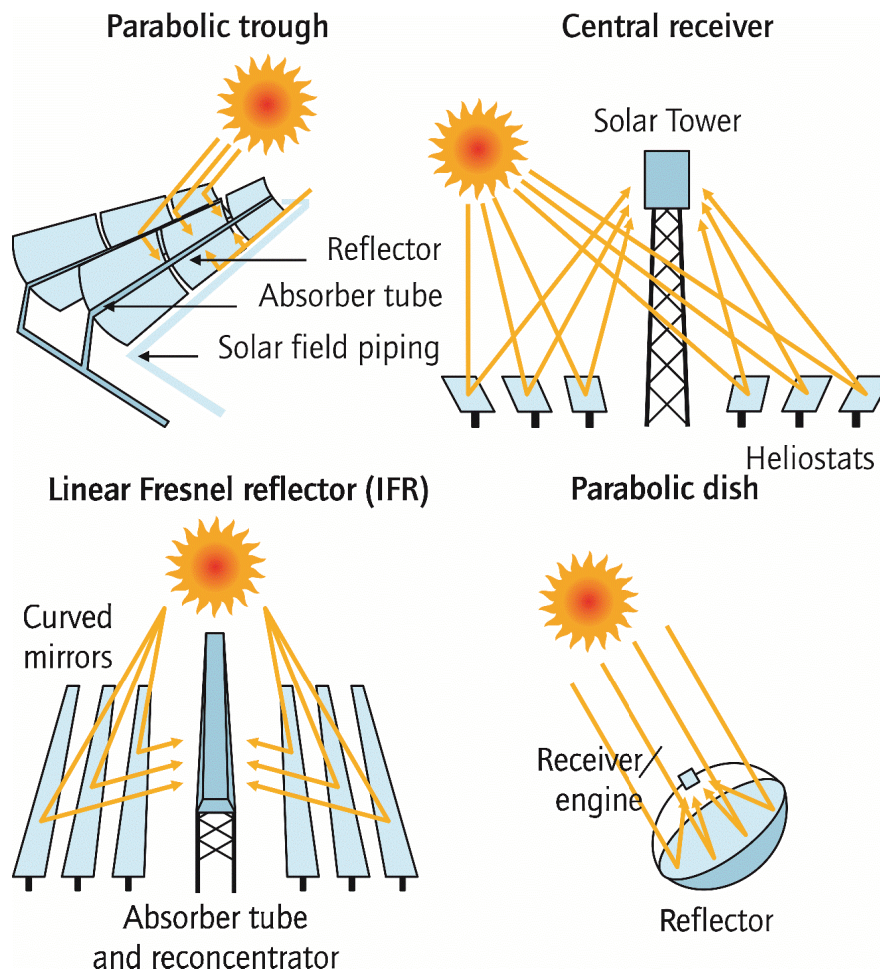
Figure 3: Overview on Concentrating Solar Power Technologies [3]

$$\eta_{max} = \eta_{th,Carnot} * \eta_{absorber}$$

Solar Tower

Parabolic Trough

Flat Plate

η_{max}

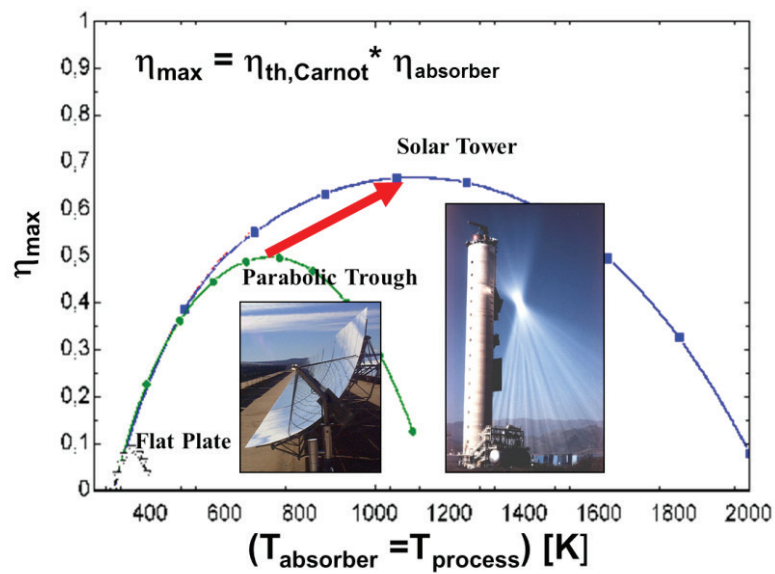$(T_{absorber} = T_{process})$ [K]

Figure 4: Theoretical process efficiencies of solar technologies

Simple thermodynamic considerations reveal that the higher the concentration level, the higher the achievable overall conversion efficiency, accompanied by higher optimum process temperature. This behavior is shown in Fig. 4. Due to the higher concentration level of solar tower systems (as a point focus system), higher process temperatures can be achieved compared to line focus systems like Parabolic trough and Linear Fresnel. As a consequence, more efficient power cycles can be applied, resulting in a higher overall conversion efficiency in solar tower plants.

Solar tower systems offer a high cost reduction potential, according to several studies [4][67]. This is already reflected in the increasing market share of solar towers for plants that were recently commissioned, they are under construction or are announced. By the end of 2013 a total solar tower capacity of 104MW was online, corresponding to 3% of the total CSP capacity. The Ivanpah plant with 377MW was commissioned in February 2014, and further plants with a capacity of 210MW are under construction with completion expected in 2014. Fig. 5 shows the increasing share of solar tower systems in the future. For the CSP projects under development almost 50% are planned as solar tower plants.

Operation   **Construction**   **Development**

- Solar tower
- Parabolic trough
- Linear Fresnel
- Dish
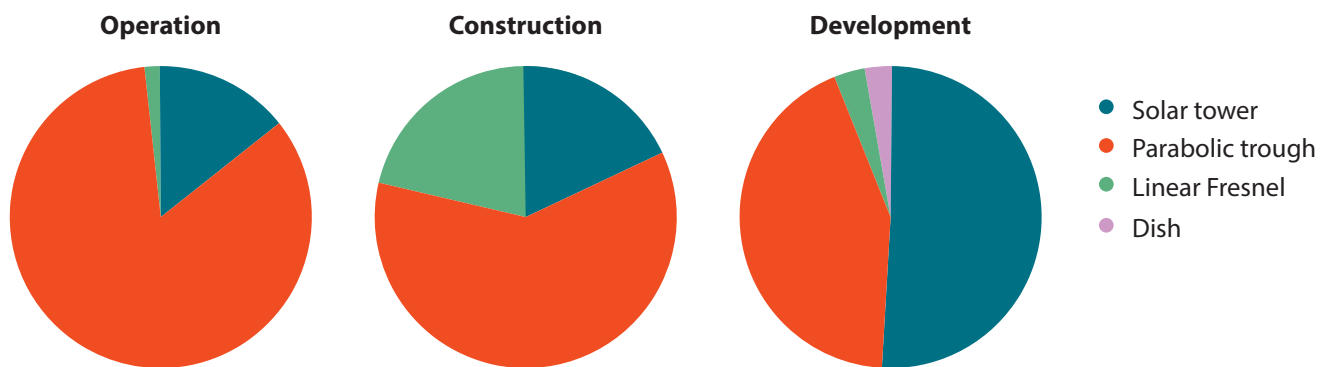
Figure 5: CSP share by technology ([2]; status 08-03-2014)

1.2 SOLAR TOWER TECHNOLOGY

A state-of-the-art solar tower plant consists of the following main components:
- **Heliostat field**: Consisting of a large number of heliostats, tracking around two axes, to reflect the solar radiation always onto the receiver; the heliostats are built from one or multiple mirror facets, usually with backsilvered low iron glass as reflector material; for higher concentration, the mirror facets are slightly curved.
- **Receiver**: In the receiver the concentrated solar irradiation is absorbed and converted into heat; the absorbed heat is transferred to a heat transfer fluid (HTF), typically water/steam, molten salt or

air which is heated up to more than 500℃; most receivers use metallic tubes, irradiated from the outside, with the heat transfer fluid passing through the tube. Ceramic materials are usually used for temperatures significantly above 500℃
- **Tower**: The tower carries the solar receiver on top.
- **Thermal storage**: Sensible or latent heat storage systems are applied; during solar operation the storage is charged by the oversized solar collection system; when no or insufficient solar energy is collected the storage can be discharged to power the thermal cycle for electricity production.
- **Power block**: The power block is similar to conventional thermal power plants (Rankine cycle, superheated steam), but smaller in power level.

The design of the power block is adapted to the specific operation conditions of the solar system. Wet, dry or hybrid cooling techniques are applied.

A scheme of a solar tower plant with molten salt as HTF is shown in Fig. 6.
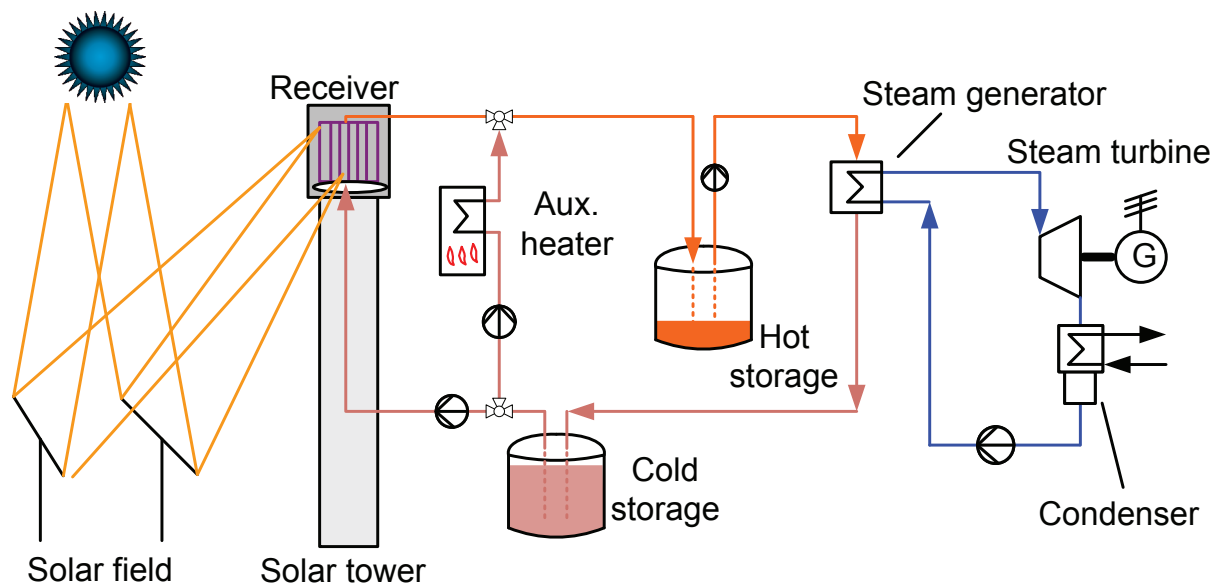
Figure 6: Scheme of a solar tower system

The key technical parameters of state-of-the-art commercial solar tower systems are:

- A **concentration factor** in the range of 500 to 1000
- **Receiver temperatures** (outlet) of 565°C (molten salt) or ~550°C (superheated steam)
- Annual **solar-to-electric efficiency** in the range of 15 to 18% (up to 30% under design point conditions)
- Thermal **storage**: capacity can be designed according to requirements (from no storage up to capacity factors of over 90%); storage efficiency > 95%
- Field layout (surround / south for Brasil)

The main differences of solar tower systems, compared to other CSP technologies, are in the following aspects:
- Higher temperatures in the receiver, and consequently in the storage

- More efficient power cycles, due to higher process parameters
- Larger temperature spread in the storage, i. e. less storage mass for a given storage capacity
- The course of the annual power production is more homogeneous, i. e. the difference between summer and winter daily production is less pronounced
- The heliostat field has usually a layout that is close to a circle; large power plants are normally built with a surround field (i. e. the heliostats are all around the tower); for smaller systems a south field arrangement is also possible (southern hemisphere, e. g. Brazil)
- The heliostat field does not require extensive land preparation, it can even be built on somewhat sloped terrains
- The high tower might interfere with other interests, e. g. air traffic; the glare from the receiver is also visible over long distances

A comprehensive literature review on solar tower systems is given by Behar et al. [7].

Solar tower layout example for Brazil

For the description of the daily and annual performance characteristic of a typical solar tower plant in Brazil, a layout was made using the layout tool HFLCAL [21]. The layout was made for 10° southern latitude, which is in the region with the highest annual DNI values in Brazil.

It should be noted that this layout is just an example for a typical plant. For a specific plant, an optimized layout has to be made taking into account the specific conditions of the project. The exemplary layout resulted in the following plant specification:

Table 2: Specifications for typical solar tower plant in Brazil

solar tower system configuration:	molten salt system
heliostat field	surround field
heliostat size (width/height)	9.57m / 12.93m
reflecting heliostat area	121m²
average reflectivity (incl. dusting)	88.4%
beam error (sunshape, slope & trackingerror)	3.664mrad
receiver	
type:	external, cylindrical, tube receiver
diameter/height:	20.14m / 22.97m
inlet/outlet temperature:	295°C / 565°C
thermal power (DP):	682MW
tower height / diameter:	283m / 25m
plant solar multiple:	3 (corresponds to a storage capacity of about 15h)
nominal electric power output	100MW
power block efficiency	44%
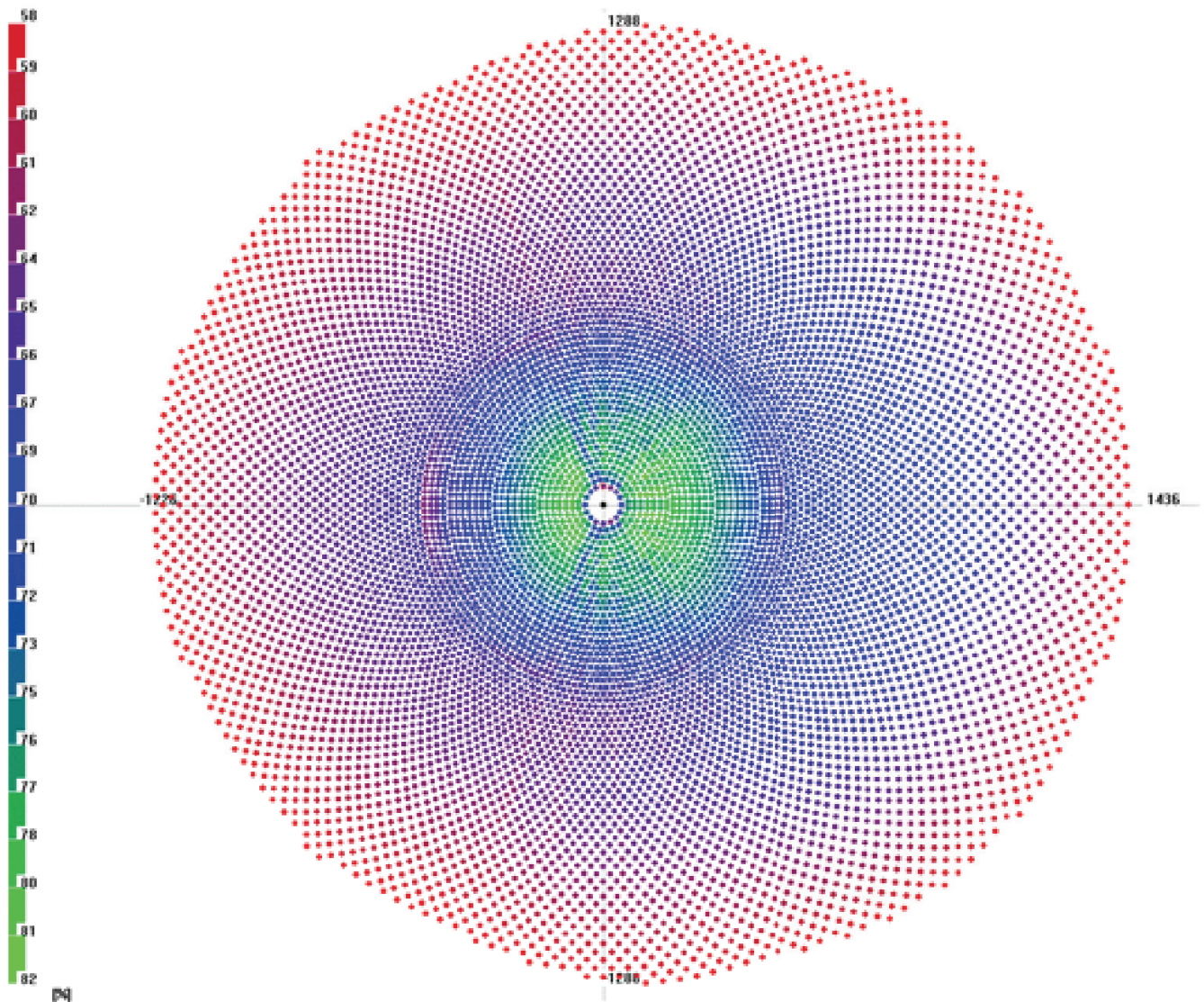
Figure 7: Heliostat field configuration for 100MW plant with 15h storage (south towards right)

The corresponding heliostat field layout is shown in Fig. 7. As the latitude of the chosen site is relatively close to the equator on the southern hemisphere, the optimum field resembles a surround field with slightly more heliostats positioned on the south side of the field. The colors of the heliostats correspond to their annual efficiency, with the scale shown on the left.

Fig. 8 shows a waterfall diagram for the specific efficiencies of a solar tower plant in Brazil. The efficiencies were evaluated for design point (DP) conditions. As design point, solar noon on March 21 (equinox) was chosen. The most significant loss is the cosine loss, caused by the fact that only the projection of the mirror area is active, and most heliostats are orientated at a certain angle to the sun's position. Other significant loss contributions are from the limited reflectivity of the mirrors and the receiver efficiency, followed by atmospheric attenuation between the heliostats and the receiver. Intercept losses (so-called "spillage"), blocking and shading have only minor contributions to the losses. The receiver efficiency is dominated by the solar reflection loss (7%), followed by thermal radiation and convection losses.
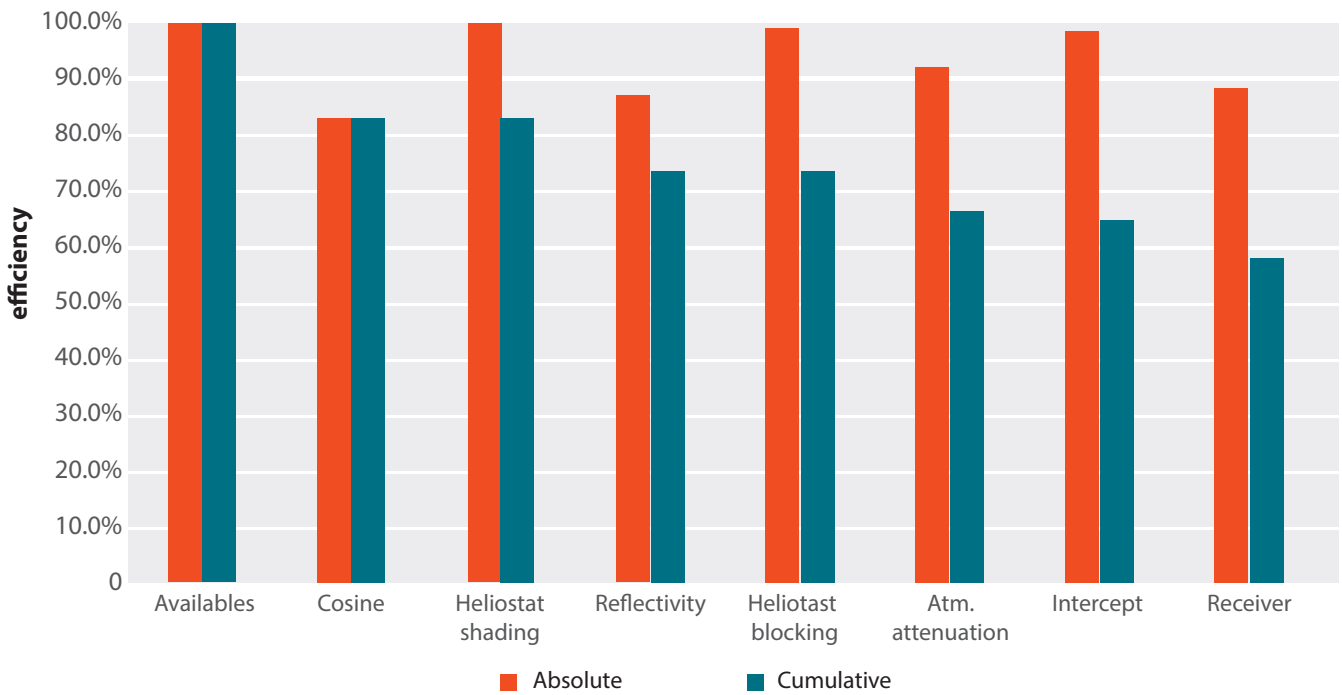
Figure 8: Design point efficiencies of a solar tower system in Brazil

The daily power characteristic of the heliostat field is shown in Fig. 9 for equinox and summer and winter solstice. The corresponding thermal receiver power is shown in Fig. 10. In the course of the day there is a pronounced variation in the thermal power output, with a sine-like characteristic peaking at noon. It is also obvious that the daily power does not differ very much with the season.
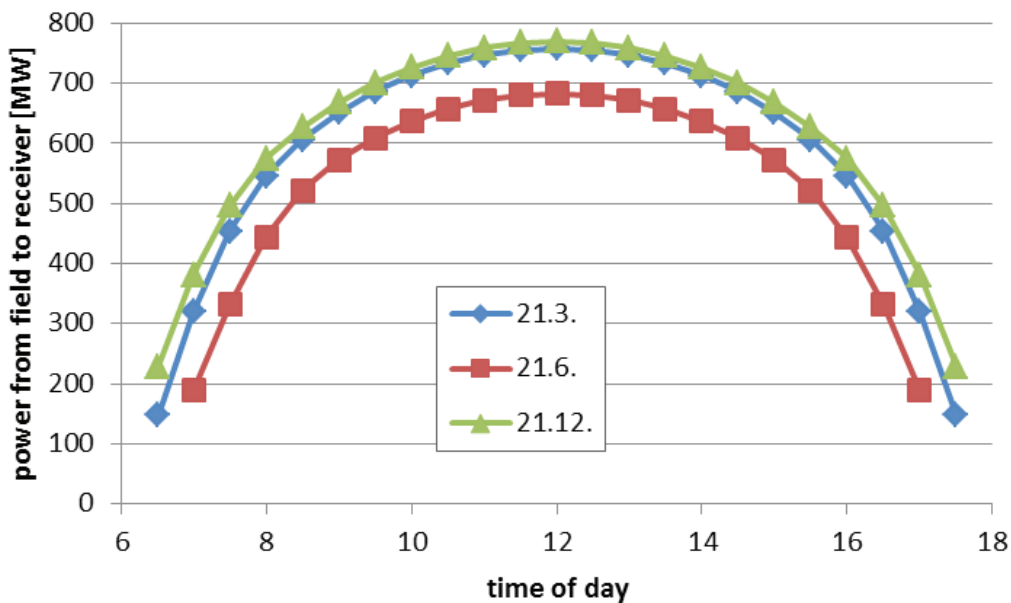
Fig. 9: Heliostat field power to receiver as function of season and time of day
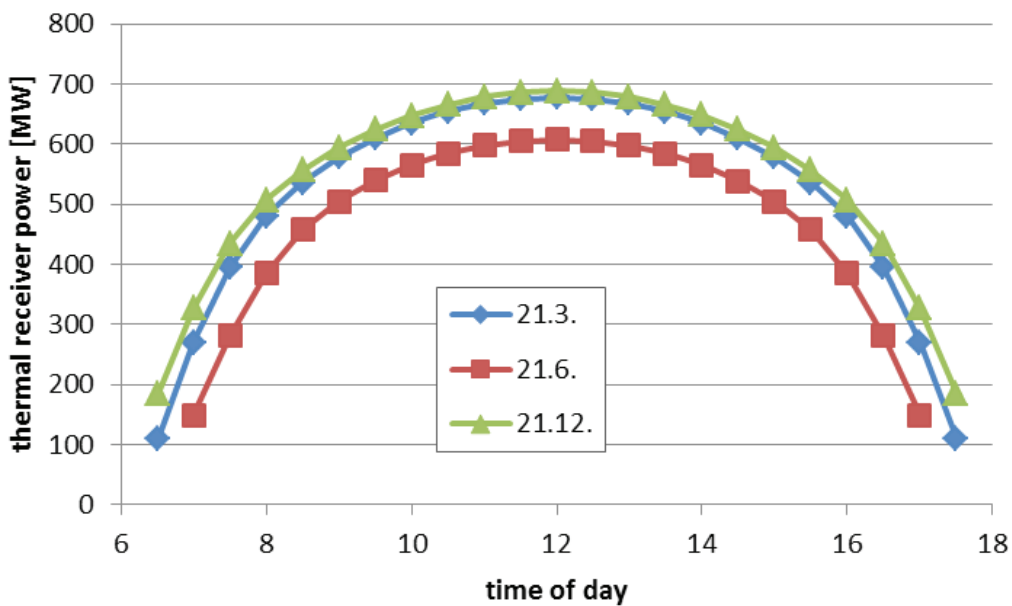
Figure 10: Receiver power as function of season and time of day

It is important to note here that for systems with storage the produced thermal power does not correspond to the power fed into the power cycle. In such systems the power cycle is designed for a nominal electric power that can be generated with a fraction of the receiver design power Pth, DP. The excess thermal power is used for charging the storage. The oversizing of the heliostat field is usually expressed by the so-called "solar multiple" (SM) that is simply the ratio Pth, DP/Pth, cycle.

1.3 HISTORY OF SOLAR TOWER TECHNOLOGY

The technological and economic potential of solar tower systems was recognized very early in the development of CSP systems. Therefore, several institutions and companies started the development of solar tower systems. Starting around 1980, several test or demonstration solar tower systems were erected, namely:
• Plataforma Solar de Almeria (PSA), Spain: Two solar tower systems were installed, with thermal power levels of about 5MW and 2.5MW (Fig. 11)

• CNRS test facility in Targasonne/France
• Solar Tower at Weizmann Institute of Science, Rehovot (Israel)
• NSTTF (Sandia, Albuquerque, USA): Solar tower test facility with 5MW thermal power
• Solar One (Daggett/USA): Once-through superheated steam receiver with power cycle, 10MWe
• Solar Two (refurbishment of Solar One): Demonstration of molten salt system with storage, 10MWe (Fig. 12)

Figure 11: Plataforma Solar de Almeria, Spain, with 2 solar tower systems

Figure 12: Solar Two: Molten salt demonstration system

Despite several approaches to build a commercial solar tower system, it took until 2007 when the first commercial solar tower plant, Abengoa's PS10 near Seville in Spain, started operation. Since then, only a few commercial plants were put into operation:

• PS20, 20MW, aside of PS10
• Gemasolar, 19.9MW, near Seville, Spain
• Sierra SunTower, 5MW, near Lancaster/CA (USA)
• Ivanpah: 377MW, Ivanpah Dry Lake /CA (USA)

More details on these plants are given in the chapter 7, together with information on other plants that are under construction or planned. Besides the commercially operated plants, a number of demonstration plants with small power levels were erected. An overview over these demonstration systems is also given in the above-mentioned chapter.

2 DETAILED TECHNOLOGICAL DESCRIPTION

This chapter gives a detailed description of solar tower systems and their main components. Different technological options are presented and discussed.

2.1 HELIOSTATS

Short Summary:
- Heliostats are reflectors that redirect the sunlight onto the receiver.
- They must be oriented very precisely.
- Mirrors must have high reflectivity and durability.
- Low costs are essential for competitiveness.

Introduction

Heliostats provide the fuel for solar tower systems. Heliostats are named "helio" for sun and "stat" for the fact that the reflected solar image is maintained at a fixed position over the course of the day. They are nearly flat and tracked mirrors (some curvature is required to focus the sun's image) that collect and concentrate the solar energy on a tower-mounted receiver. Comprehensive overviews on past, current and future heliostat technology are given [9][10]. Fig. 13 shows the second generation heliostat of Brightsource Energy.
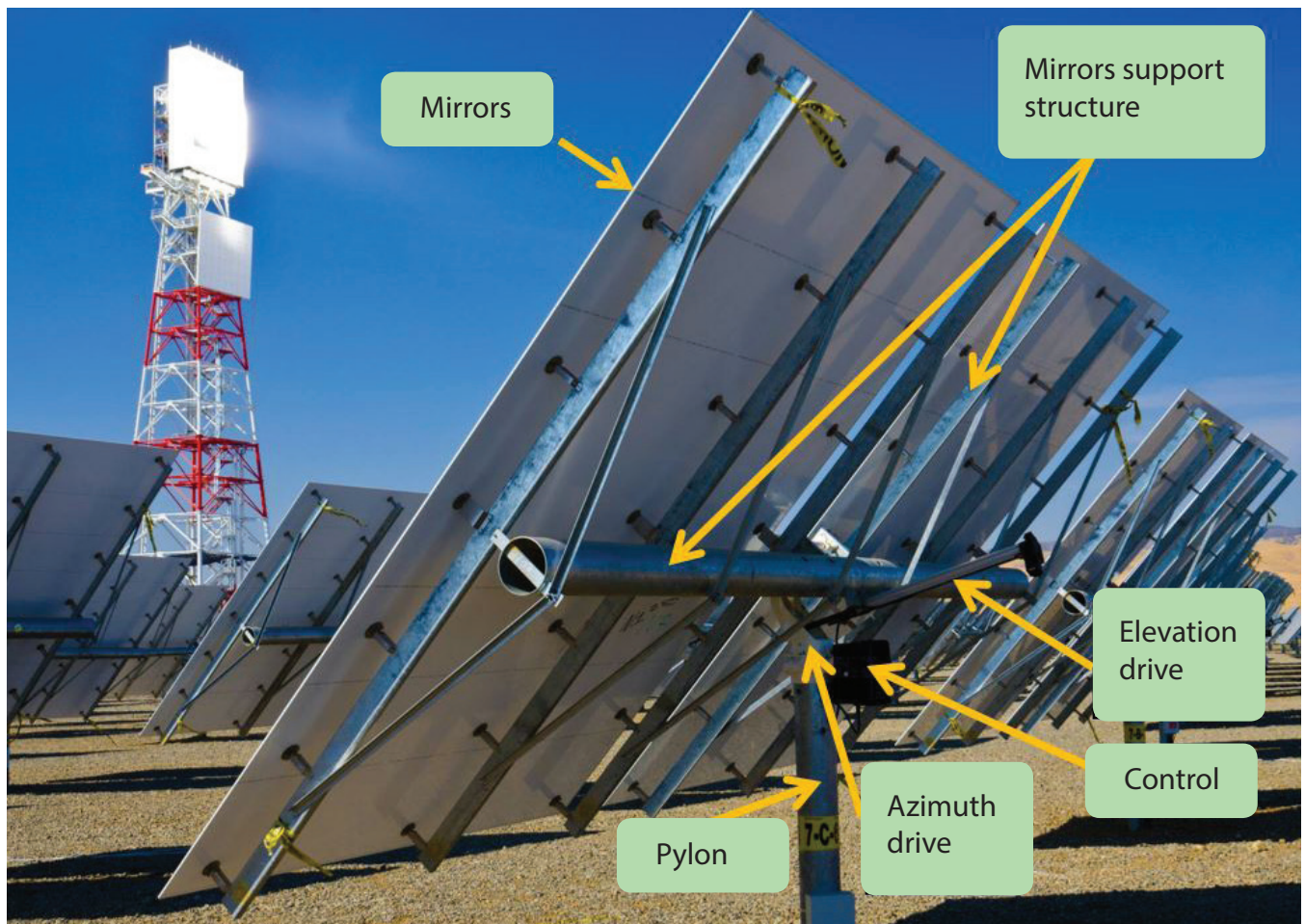
Figure 13: Heliostat and its components [Brightsource Energy]

To maintain the sun's image on the solar receiver, heliostats must track at all times in such a way that the reflected image of the sun is positioned on the receiver. The major components of a heliostat are shown in Fig. 13 and are described briefly below. These components are the mirrors, the mirror support structure, the pylon and foundation, the tracking control system, and the drives.

Power towers must have low capital and O&M costs in order to compete with the relatively low cost electrical power produced from other sources such as hydro power. The heliostats currently represent about 40% of the capital cost of a central receiver power plant. The relative fraction of the total cost of a heliostat of its major components is shown in Table 3 below.

Table 3: Heliostat component costs

sub function	component	cost share
reflect sunlight	mirrors	25 - 30%
fix shape of reflective material	mirror support structure	15 - 20%
connect system to ground	pylon, foundation	10 - 15%
determine offset of mirror plane orientation	position sensors, control	5 - 10%
rotate reflective material about two axes	drives	30 - 35%
	assembly, installation	10 - 15%

Heliostat design characteristics

Axis orientation

Different options for the orientation of the heliostat rotation axes exist. These are described shortly below.

Azimuth-Elevation
The mirrors are turned about the vertical first axis to follow the azimuthal movement of the sun. They are mounted on a torque tube which turns about the horizontal second axis to follow the elevation of the sun during the day. The vertical pylon and the horizontal torque tube form a "T". Therefore this kind of heliostat is often called "T-type heliostat".

Figure 14: T-type heliostat with azimuth-elevation axis orientation

Target aligned

Parabolic shapes reflect rays to their focal point – but only if the rays are parallel to their optical axis. For other directions the focal spot is widened. This optical error called "astigmatism" can be reduced if the rays are lying always in one certain plane perpendicular to the mirror plane. This is the case when primary rotation axis ("spin axis") is aligned towards the receiver (Fig. 15). For small power plants with big heliostats the gain in efficiency is significant. But especially for small power plants usually small heliostats are used and then the gain is only a few percent [11] while the extra effort for the alignment of the primary axis to the target is significant.
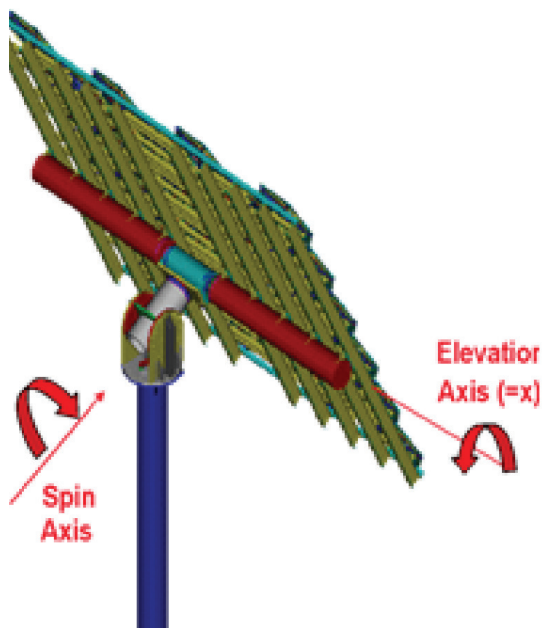
Figure 15: Heliostat with first axis aligned in direction to the receiver (target)

Horizontal first axis

The optical loss of heliostats can be reduced by reducing the distance to the receiver. This can be achieved by a higher field density. For conventional azimuth-elevation and for target aligned heliostats the diagonal of the mirror plane defines the minimal distance between the heliostats to exclude collision. For heliostats with horizontal first axis the heliostats can be positioned closer to each other because they do not rotate around the vertical axis (Fig. 16). Thus the minimal distance of the heliostats in direction of the horizontal axis is not the diagonal but the chord length of the mirror plane. The gain in efficiency is only about one percent. So the main advantage of this concept is the possibility to use linear drives or rim drives (see next paragraph).
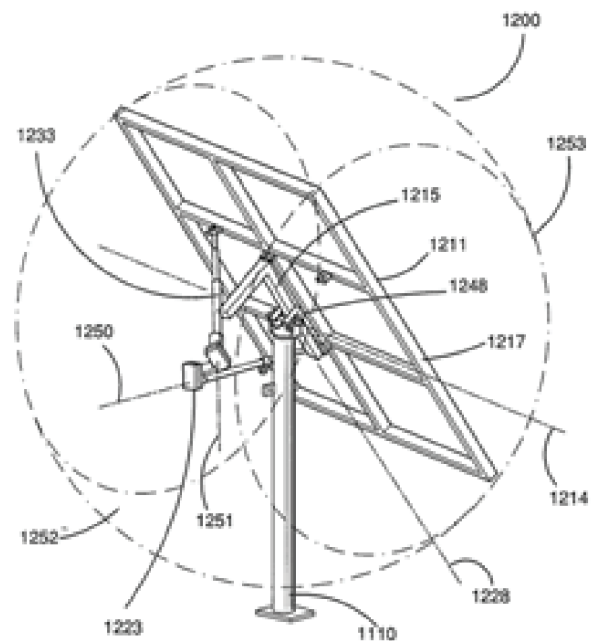
Figure 16: Space of motion of heliostats with horizontal first axis [12]

Drives

Slew drives

For the azimuthal movement usually slew drives are used. They are self-locking, precise, can resist high loads and allow an angle range of 360°. However, they are relatively expensive.

Linear drives

For the elevation movement usually linear drives are used because they are cheaper than slew drives. The backlash can be compensated by pretensioning via the gravity load of the mirror panel. For the azimuth axis at conventional azimuth-elevation heliostats one linear drive would not be sufficient because the needed angle range is too high. But, at heliostats

with horizontal first axis (Fig. 17) an angle range of only 120° or less is needed also for surround fields. For the second axis a pretensioning by the gravity load is not possible and therefore the backlash has to be lower than for the first axis.

Figure 17: Heliostat with two linear drives and horizontal first axis [13]

Rim drives
The lever arm of the actuators is increased at heliostats with rim drives (Fig. 18). By this approach, simple and inexpensive low torque and low precision gears can be used. The rims can be driven via chains, traction sheaves or simply by winch wheels [14].
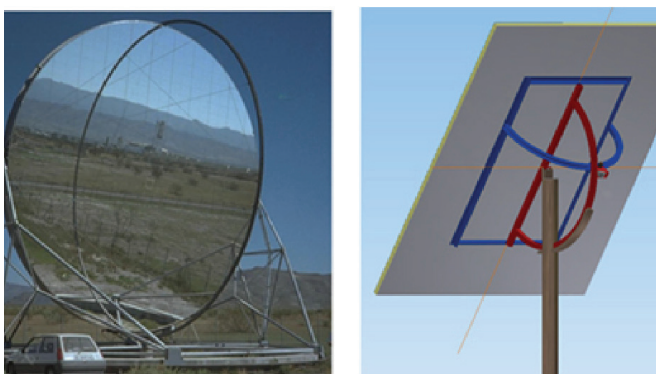
Figure 18: Heliostats with rim drives

Hydraulic drives
Hydraulic drives promise to be a cheap solution for big heliostat sizes [15]. They also can be used as azimuth drive, but then an extra mechanism to transform the linear movement into rotation is needed for the complete required angle range of T-type heliostats (Fig. 19).
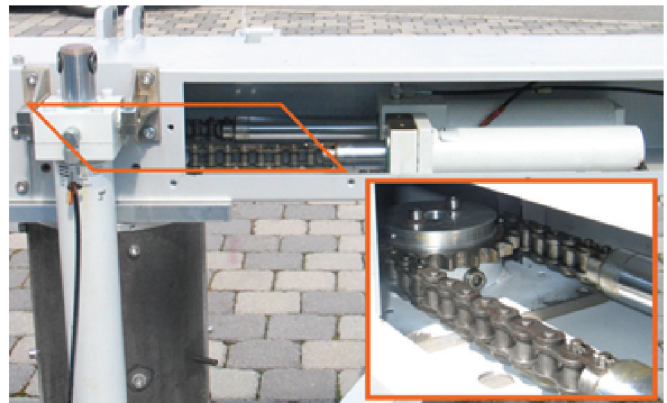
Figure 19: Hydraulic azimuth drive

Mirror facets

Material
Currently back-silvered glass mirrors are the preferred solution, because of their stability against degradation. Thin glass mirrors (~1mm) provide higher reflectivity, but require an additional support structure. Thick glass mirrors mirrors (~4mm) are self-supporting and can be fixed with few attachment points. Alternatives are aluminum sheets and metalized polymer films. Drawbacks of the alternatives are the lower reflectivity and the need for additional coating against abrasion by sand and cleaning. The cost reduction of the material must be higher than the loss in reflectivity times the specific cost of the complete heliostat.

Pads
Usually 3-4 mm thick glass mirrors are used. Ceramic pads with same thermal expansion ratio as glass are glued onto the mirrors. These pads are connected to the support structure by flexible elements which compensate the differences of thermal expansion of the glass mirrors and the steel support structure

(see Fig. 13). The pads must be mounted slightly rotatable to ensure that no additional tensioning of the glass is caused by the pads which would increase the risk of breakage.

Sandwich structure
Sandwich facets have several advantages: thin glass mirrors of about 1mm thickness with about 2% higher reflectivity can be used, the total weight is lower, the shape accuracy and stiffness is very high and the mirror breakage is very low [16]. The slope error caused by different thermal expansion coefficients of a steel back layer compared to a glass front layer can be reduced to an acceptable value if a thickness of the core material of a few centimeters is provided. The challenge is to find a cheap but durable and precise solution.

Stretched membrane
High accuracy and reflectivity can also be reached by thin glass mirrors on stretched membranes (Fig. 18, left). However, the extra expense for the ventilation system to induce the needed pressure difference and the relatively small weight reduction might be main reasons why this approach is no longer pursued [17].

Energy supply

In current heliostat systems, energy supply and communication is realized by wires. The cost of wiring [17] can be avoided by autonomous heliostats, provided with photovoltaic cells, electric energy storage and wireless communication [18]. The cost of wiring is significant especially for (many) small heliostats, and when the legal requirements demand placing the wires deeply in the ground. A further advantage of autonomous heliostats is that lightning protection is not necessary, because only single heliostats would be affected by a lightning strike and not the complete field.

Size

The question on the cost optimum size cannot be answered yet. It depends on the production rate, the kind of ground and related foundation and the specific cost of the different components. Small heliostats are lighter because of the following: By increasing the edge lengths of the mirror panel the mirror area increases by the same ratio to the power of two. All other dimensions of the heliostat must be increased by the same ratio as the edge length to keep the bending stress constant. Therefore, accordant to [17], A.3, the mass of the heliostat increases by trend with the edge length to the power of three or with the mirror area to the power of 1.5 respectively (dependency of the wind speed with height neglected). Hence, small mirror support structures are advantageous due to their lower specific weight, as the weight is a measure for the cost especially for high production rates. In contrary, larger heliostats have the advantage that less foundations, wiring, control units and drives are needed.

Heliostat errors

Important characteristics of a heliostat are the slope error and the tracking error.

Slope error
For an ideally shaped parabolic mirror panel parallel rays (in direction of the optical axis) would all be reflected to one certain focal point. With real mirrors only a focal spot of a certain size can be realized. The flux density is approximately Gaussian distributed within this spot. A measure for the spot size is the standard deviation of the flux distribution. Roughly said, the standard deviation is one third of the focal spot's radius. To be independent from the distance the slope error is not given in length units but in angle units. A typical slope error value of a good heliostat is about 1 mrad.

Tracking error

The tracking error gives information about the accuracy of the drives and the control. It can be determined by measuring the distance between the center of the focal spot and the aim point (where the center of the focal spot should be) for a sufficient amount of points in time. The distribution of distances is then fitted to a Gaussian distribution to determine the standard deviation. The value is transformed from length units to angle units. A typical tracking error value for a good drive system is 0.6 mrad per rotation axis.

Wind resistance

Heliostats of central receiver solar power plants are exposed not only to the sun but also to the wind. The layout of the foundation, the structure and the drives have to consider the maximal wind loads that are expected to occur. For storm conditions the mirror plane is oriented horizontally to achieve the lowest area of wind attack. The wind loads are determined by wind tunnel tests [19](Fig. 20). Investigations on the dynamic wind load shall help to be able to reduce the wind loads in future for example by shock absorbers or by kind of spoilers [20].
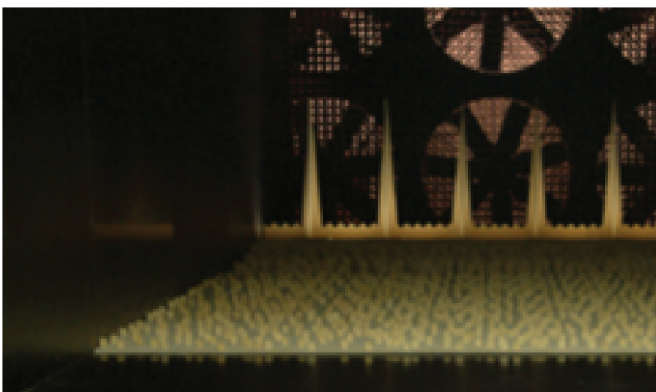
Figure 20: Determination of wind loading by wind tunnel tests

Rotation speed

In case of problems the heliostat must be able to remove its focal spot fast enough from the receiver to avoid overheating of the receiver (this is called "defocus"). Furthermore it must be fast enough to be able to reach stow position (horizontal mirror plane) in case of increasing wind speed before the wind speed reaches a critical value. A typical value for the rotation speed of the drive is 9°/min which means stow position can be reached within 10 min.

2.2 HEAT TRANSFER MEDIUM

Short Summary:
- The heat transfer medium is heated in the receiver and transports the thermal energy. to the power block and/or storage.
- It must be stable and should not cause degradation (corrosion).
- Current commercial solar tower systems use water/steam or molten salt as HTM.
- Future systems might use advanced HTM for increased working temperatures.

The heat transfer medium of a solar tower plant has a significant influence on the system configuration and the components. The receiver on top of the tower is converting the concentrated solar radiation into thermal energy. The heat transfer medium is heated in the receiver and is transferring the thermal energy to the power block and/or the storage. When the heat transfer fluid is also the working fluid of the power cycle (i. e. in water/steam systems) no heat exchanger is required. When the heat transfer fluid is different (i. e. in molten salt or air systems) a heat exchanger is necessary to introduce the heat into the power cycle.

The heat transfer medium can be gaseous, liquid or solid. **Gaseous heat transfer fluids** (air, helium, CO_2) offer a large temperature range for operation. They can be used from ambient temperature with practical no limitation for the upper temperature. In this case only the receiver material is the limitation for the upper temperature. As there is no phase change within the operating temperature range the fluid properties are relatively constant (no sudden change of density as for water/steam). A major disadvantage of gaseous fluids is the low heat transfer coefficient caused by low density and low thermal conductivity, resulting in over temperature in the receiver. The heat transfer can be improved by higher velocities in the receiver, at the expense of higher pressure drop. Increasing the system pressure improves the heat transfer capability due to the higher density of the fluid. Receivers using gaseous fluids under pressure have to be treated as pressure equipment.

Liquid heat transfer fluids offer a significantly higher heat transfer capability than gaseous fluids. This means usually smaller and more efficient receivers. Depending on the type (molten salt, liquid metal) there is a lower and upper limit for the operation temperature. The lower limit is defined by the freezing temperature when the liquid is changing to the solid phase. The upper limit is indicated by the temperature where the fluid itself becomes instable (chemical reactions, decomposition, evaporation).

Phase changing heat transfer fluids are subjected to a phase change within the working temperature range. This is the case for water/steam systems. The receiver is first heating the liquid water until saturation temperature, then the water is evaporated and the generated steam is then superheated. The steam can be used directly to drive a steam cycle. In this case there is no need for a heat exchanger between receiver and power block. The significant changes of the fluid properties in the evaporation section lead to more complex receiver operation mainly in transient situations (start up, clouds).

Solid heat transfer media are realized for example by small solid particles. For solar purposes ceramic particles (e.g. bauxite) with a diameter of about 1mm are proposed to be used both as heat transfer and storage medium. In comparison to liquids there is no phase change over a wide temperature range. Also, there is no lower temperature limit. Special cases are small carbon particles entrained in air, that react during the heating process and result in a hot air stream, i. e. a gaseous heat transfer fluid.

The following table gives an overview over some used and proposed heat transfer media:

Table 4: Properties of typical heat transfer media

	Tmin [°C]	Tmax [°C]	thermal conductivity [W/mK]	volumetric heat capacity [kJ/m³K]
air	-	-	0.059	0.2
helium	-	-	0.32	3.0
solar salt	220 (m.p.)	~ 565	0.55	2675
sodium	98 (m.p.)	883 (b.p)	64.9	1042
lead-bismuth eutectic	125 (m.p.)	1553 (b.p)	14.9	1415
solid particles	-	> 1000	6.7	3560

(m.p. = melting point; b.p. = boiling point at standard pressure)

In commercial solar tower plants, currently only two heat transfer fluids are used: Water/steam and molten salt ("solar salt").

Water/steam is used in the commercial solar tower plants PS10/PS20 and the Ivanpah plant. It is also foreseen for the Khi Solar One plant, currently under construction. The produced steam is used directly in the steam cycle. The water/steam is preheated, evaporated and superheated in metallic tubes in the receiver. Current water/steam systems have no or only little storage capacity installed, as there is no cheap and efficient storage technology available today.

Molten salt ("solar salt", a mixture of 60% NaNO3/ 40% KNO3) is used in the commercial solar tower plant Gemasolar, as well as in the plant Crescent Dunes currently under construction and to be commissioned in 2014. It is also foreseen for the recently announced solar tower plant in Chile. This salt has a melting point of 220°C and is heated up to 565°C. At higher temperatures the salt mixture starts to decompose. As solar salt is relatively cheap it can be used also as storage medium, i. e. no heat exchanger is required between the receiver loop and storage. Molten salt shows good heat transfer coefficients in the receiver, and allows therefore for small and efficient receivers with limited over temperatures. The temperature range of molten salts fits well to common steam turbines. Another advantage is the existing industrial experience with using molten salt as heat transfer medium in chemical and metal industry. The high melting point of 220°C is a disadvantage of this heat transfer fluid. As solidification of the salt must be avoided in the receiver and all other components, all these components must have an additional heat tracing to prevent salt freezing. In current solar tower designs the receiver is drained during non-operation periods.

Liquid metal offers very high heat transfer coefficients, resulting in lower temperature differences and higher acceptable solar flux densities in the receiver. For this reason the receiver can be smaller. The lower melting temperature, compared to solar salt, promises reduced parasitic power for heat tracing. There exists a lot of experience from the nuclear sector using liquid metals as heat transfer medium. Currently, the main disadvantage of liquid metals is the lack of an appropriate storage configuration.

Air as heat transfer fluid has some advantages over other fluids. It is available with no additional costs. It has no temperature limitations (no freezing, no decomposition) and it is environmentally harmless. The main disadvantage is the low heat transfer capability leading to large receivers when tubes are used. In volumetric receivers this is compensated by the small structures that enhance the heat transfer.

Solid particles offer an extensive temperature range, from ambient conditions up to 1000°C e.g. for industrial grade bauxite. Less expensive particles (e.g. sand) are a candidate for lower-temperature applications. The particles can be heated directly by the concentrated radiation, thus improving the performance and reducing costs of the solar receiver. The same particles can be used directly as storage material. Particle transport and heat exchanger technologies are open issues for such high temperature particle systems.

Summary of heat transfer media:

The following table gives a comparison of the heat transfer media options.

Table 5: Summary of heat transfer media

	Heat transfer	Temperature range	price	Environmental hazard	remarks
air	bad	good	good	no	
water/steam	good	average	good	no	
molten salt	good	average	average	no	can be used as storage medium
liquid metals	excellent	good	bad	potentially	
solid particles	good	excellent	good	no	can be used as storage medium

2.3 RECEIVER

Short Summary:
- The receiver absorbs the concentrated sunlight.
- The absorbed solar radiation is converted to heat that is transferred to the HTM.
- Actual commercial receivers use panels with multiple tubes.
- Future receivers might use direct absorption for increased temperatures at high efficiency.

So called receivers are converting the concentrated solar radiation to high temperature heat and transfer the heat to a working medium. The design of such receivers can be more or less simple like tube receiver's or more complex like pressurized volumetric receivers. In general, receivers can be classified into two main groups:
- External receivers: The absorbing elements are installed on the outer side of a structure (e.g. a cylinder); this design is usually applied with surround fields
- Cavity receivers: The absorbing elements are installed inside a cavity, with the cavity aperture being smaller than the internal absorber surface; this design is usually applied with north or south fields (on northern or southern hemisphere, respectively)

Receiver types can be also categorized by the way the concentrated solar radiation is absorbed and transferred to the heat transfer medium. Two categories exist:
- Indirect absorption receivers: The solar radiation heats an absorbing surface (e.g. a tube), the heat is then transferred via conduction and convection to a heat transfer medium
- Direct absorption receivers: The solar radiation is directly absorbed in the heat transfer medium (e.g. in solid particles)

As the receivers are exposed to high solar flux densities in combination with high temperatures, the requirements are quite high. The receiver should
- convert and transfer the heat with high efficiency
- accept high and inhomogeneous heat fluxes (locally and in time)
- achieve long lifetime at acceptable costs

To fulfil these needs the design of receivers has to take care of several thermal and mechanical boundaries. Heat transfer by convection, conductivity and radiation exchange has to be considered simultaneously. Receivers for central tower solar plants work at high concentrating solar heat fluxes and at high temperatures. The load situations are quite complex. The solar heat flux varies over time of day and year leading to different load situations. Fast transients can occur by clouds blocking the sunlight totally or partially. This leads to high and alternating stresses in the materials that affect the lifetime of the receiver. The thermal efficiency of the receiver is strongly influenced by the temperature and the average flux density on the receiver. The (over) temperature of the receiver is mainly influenced by the used heat transfer medium. Liquid heat transfer fluids allow for a smaller receiver than gaseous fluids as the heat transfer capability is higher. A comprehensive overview on current receiver technologies and future developments is given in [22].

Indirect Absorption Receivers

All current commercial receiver types belong to this group, and are built as metallic tube receivers. Multiple panels, each consisting of a number of parallel absorber tubes, are interconnected in serial or parallel configuration. Header sections are distributing and collecting the fluid. The absorber tubes are coated with a black paint, e.g. Pyromark 2500 Flat Black [23]. The fluid is passing through the interior of the tubes and is convectively heated by

the tube walls having absorbed the solar radiation on the outside. Tube receivers can be built as external or cavity receivers. In external receivers the panels are arranged in a cylindrical or polygonal configuration. In cavity receivers the tubes are arranged along the walls of an insulated cavity.

Receivers for water/steam are usually separated into several receiver zones to account for the significantly different heat transfer characteristics during evaporation and superheating. The evaporator section, also performing the preheating to saturation temperature, can accept relatively high solar flux densities. In a steam drum the remaining water is separated and the steam is fed into the superheater section. Due to the gaseous fluid (water vapour) the acceptable flux densities in this section are lower. The steam temperature and mass flow in the superheater section depends on the actual operation condition of the evaporator section. An appropriate control system must manage the number of heliostats focussed on each section according to the actual operation status.

Receivers for molten salt use multiple panels that are connected in parallel and serial mode. The panels at the inlet side are located in the receiver region where the highest flux density levels occur (e.g. on the north side of the Gemasolar receiver). Due to the lower fluid temperatures in this region higher temperature differences between fluid and tube wall can be accepted with reasonable receiver lifetime. The higher the fluid temperature rises, the lower the acceptable fluxes get. Test segments of advanced tube receivers with molten salt demonstrated operation at flux levels up to 1MW/m².

Receivers using liquid metal as HTF are able to accept higher solar flux densities, and to operate at higher temperatures. Past receiver designs for liquid metal were built with metallic tubes, with the design of such receivers being quite similar to that of a molten salt receiver.

Volumetric receivers use highly porous structures for solar absorption and heat transfer. The porous absorber is usually a matrix or a foam structure made of SiC ceramic. It offers a huge internal surface area, allowing effective heat transfer. The concentrated solar radiation is absorbed in the volume of the absorber, as the porous structure allows for penetration of the radiation. Then, air or another gas is passing through the structure and is heated by forced convection. There are two main directions of volumetric receiver concepts under development. An open volumetric receiver uses ambient air as heat transfer fluid. The hot air can then be used to produce steam in a steam generator. If the fluid is under pressure a so-called pressurized volumetric receiver can be used. Such a receiver consists of an internally insulated pressure vessel, the porous absorber and a transparent quartz window covering the vessel's aperture. As the quartz window is limited in size, it is necessary for high power levels to connect several receivers to a cluster. For a complete coverage of the focal spot, secondary concentrators with hexagonal entry apertures in front of the receivers are used.

Examples for receivers that are or will be in operation in commercial solar tower plants are listed below.

Water/steam receivers:

plant	PS10 / PS20	eSolar	eSolar	Ivanpah
receiver type	tube receiver, cavity	tube receiver, double cavity	tube receiver, external	tube receiver, external
receiver outlet temp.	250°C / 257°C	218°C/ 440°C	218°C/ 440°C	250°C/ 565°C
Pressure	40bar / 44bar	60bar	60bar	160bar
Thermal power	55MW / 110MW	8.8MW	8.8MW	~ 330MW (est.)
receiver area	260m² / n.k.	n.k.	n.k.	n.k.
average flux density	235kW/m² / n.k.	n.k.	n.k.	n.k.

Table 6: Overview of operational water/steam receivers

(n.k. = not known; est. = estimated)

Figure 21: PS10 receiver during installation (left); double-cavity receiver (eSolar) (right)

Figure 22: Brightsource external receiver (Ivanpah)

Molten salt receivers:

plant	Gemasolar	Crescent Dunes
receiver type	tube receiver, external	tube receiver, external
receiver outlet temp.	565°C	565°C
Thermal power	120 MW	n.k.
receiver area	n.k.	receiver diameter/height: 15.8m/35m, 14 panels, 66 tubes each, panel length/width: 22.86m / 3.35m
average flux density	~ 540kW/m²	

Table 7: Overview of commercial molten salt receivers
(n.k. = not known)
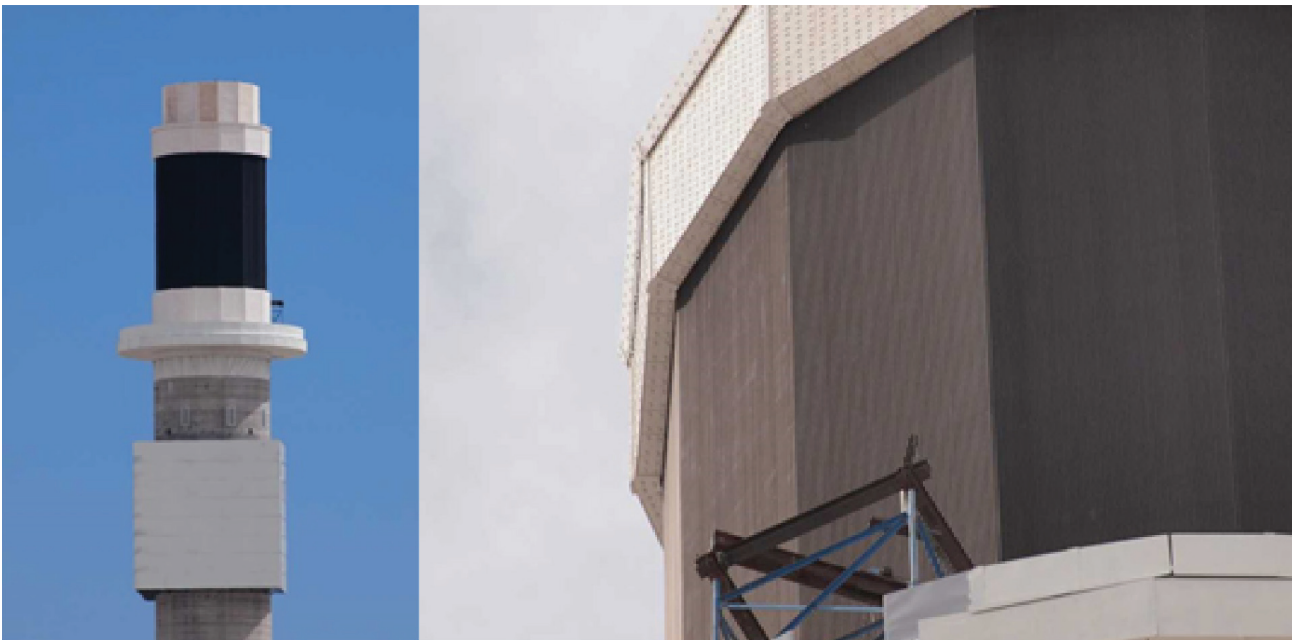
Figure 23: Molten salt receiver of Crescent Dunes plant [source: DLR]

Direct Absorption Receivers

In direct absorption receivers (DAR) the heat transfer medium also acts as the absorber. As the solar radiation does not need to heat an absorbing structure first, and then transfer the heat based on a temperature difference, the DAR concept promises lower over temperatures and reduced requirements for the receiver structural materials. DAR can use the following media:

• Gaseous fluids: e.g. air with entrained carbon particles

• Liquids: e.g. molten salt, optionally with dopants to increase absorptivity
• Solids: e.g. small ceramic particles

DAR promise to enable increased receiver temperature at reduced cost. However, the receivers are currently in the R&D phase. The focus is on receivers with entrained carbon particles (that disappear during heating) and solid particle receivers. Fig. 24 shows a conceptual design of a falling particle receiver.
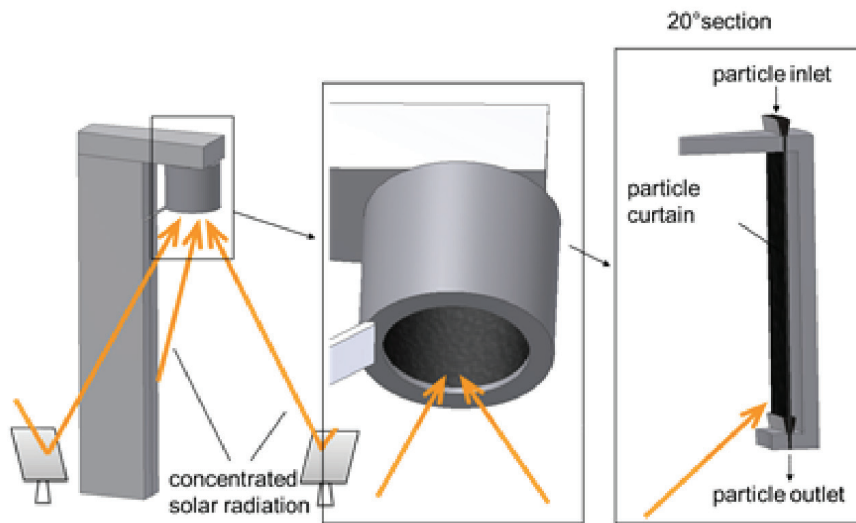
Figure 24: Falling particle receiver in face-down configuration

2.4 TOWER

Short Summary:
- The tower structure is built of concrete or a steel framework.
- High stability and stiffness under static and dynamic loads require.

The solar tower is the support structure for the solar receiver, which has to be placed at a certain height above the solar field to facilitate an efficient and optimized solar field. Depending on the design and type of the solar tower plant, the tower contains additional structures like power block components, piping and maintenance facilities.

Depending on the actual site conditions, various tower types are available, including reinforced concrete towers, lattice (framework) towers and guyed towers. Tower constructions from wind turbines are considered as well, in order to use synergies and reduce investment costs. Two examples of tower constructions are shown in the following figure.

Figure 25: Examples of existing tower constructions (left: concrete tower, right: steel tower)

The tower height and general shape has influence on the heliostat field efficiency and heat generation costs. When planning the tower construction, a set of unique considerations has to be taken into account:
- Tower shadow has (slightly) negative effect on heliostat field efficiency
- Stability against wind – movement of the receiver due to wind potentially lowers system efficiency
- Sufficient space for assembly and maintenance of the receiver and potentially other power block components located in the tower
- Possibility of "repowering" – installation of a more advanced receiver

Furthermore a set of general criteria has to be considered, including cost, stability in case of earthquakes, construction time and others.

2.5 STORAGE

> Short Summary:
> - Thermal storage enables load shifting and power generation during night.
> - Thermal storage is very efficient.
> - Storage types: Direct (HTM is also storage medium) or indirect (storage medium is different to HTM).
> - Storage size can be adapted to grid requirements.

The integration of thermal storage is a very important feature that sets CSP plants apart from most other renewable energy technologies. Thermal storage offers several advantages:
- Dispatchable electricity generation: delivery of power to the grid can be tailored according to the demand or tariff structure
- Higher system efficiency
- Thermal storage avoids transients in the power

block, e. g. from cloud passages
- Part-load operation of the power block can be avoided or reduced
- High storage efficiency: thermal storage systems reach efficiencies in the range of 95% to 99%
- Plant start-up time can be reduced by using stored energy for preheating
- Higher capacity factor: less backup capacity is required in the grid for compensation of fluctuating renewables, or backup power plants (usually with low efficiency) are used less often
- LCOE can be reduced: power block full load hours are increased, resulting in lower specific cost for this part; specific cost of other plant components remain nearly unchanged

The design of the storage system is strongly dependent on the solar collector system and the power block. Mainly the heat transfer fluid and the receiver inlet/outlet temperature determine the type and layout of the thermal storage. The key data of a storage system are:
- Type of storage system
- Thermal capacity
- Thermal power
- Operating temperatures
- Required mechanical power (parasitic loads)
- Thermal losses

The types of thermal storage systems can be categorized into sensible, phase change and thermochemical storage. In commercial solar tower systems so far only sensible and phase-change (latent) systems are used.

In solar tower systems using molten salt as the heat transfer fluid (e. g. Gemasolar), a sensible heat storage system is applied. Current designs are built as a two-tank system, consisting of a "cold" tank (containing molten salt at about 290°C; item 2 in Fig. 26) and a hot tank (containing salt at about 565°C; item 4 in Fig. 26). When the storage is charged, molten salt from the cold tank is fed through the receiver and heated up. The exiting hot salt is then

routed into the hot tank, i. e. salt inventory is heated and moved from the cold to the hot tank, changing the salt level in the tanks. During discharge, hot salt from the hot tank is routed through the steam generator to drive the power block, and the cooled salt is fed back to the cold tank, changing the salt level in the tanks in the inverse way.

The molten salt mixture ("solar salt") has a specific heat capacity of about 1500 J/kgK. With a density of about $1950kg/m^3$ and a temperature rise of 275K, a specific energy density of about $223kWh/m^3$ is obtained. In the two-tank system the corresponding volume has to be installed both in the hot and the cold tank. The two storage tanks of Gemasolar are shown in Fig. 27, located at the bottom of the tower. Each tank has a diameter of 23m and a height of 10.5m, the total salt mass in the storage amounts to 8500 tons [40].
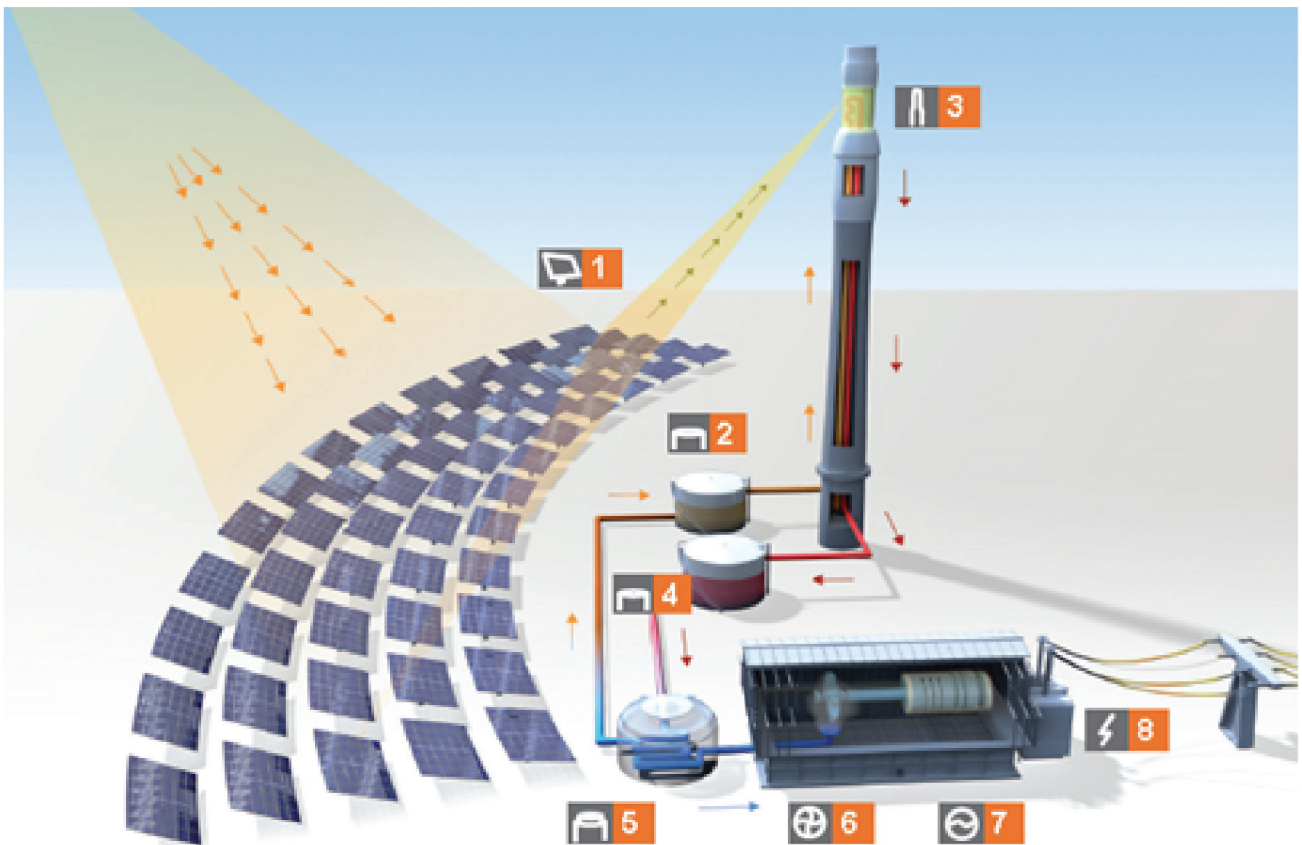
Figure 26: Scheme of molten salt storage system [24]

Figure 27: Thermal storage of Gemasolar plant (two tanks right of tower; 15h capacity)

In solar tower systems using water/steam as heat transfer fluid, only limited storage capacity is currently realized. Steam accumulators are used (so-called Ruth storage) where steam is condensed in large pressurized tanks during charging, resulting in a slight increase of (saturation) pressure and temperature. During discharge, the pressure is slightly decreased, resulting in evaporation of water and steam generation for use in the power cycle. As this type of storage system requires large hot-walled storage tanks at high pressure, the costs are relatively high. Therefore, only moderate storage capacities (e. g. 1h in PS10 /20) are realized. For future plants with water/steam receiver, new storage concepts, using either molten salt or a combination of sensible and latent heat storage, are proposed.

When air is used as the heat transfer fluid, regenerator-type storage systems are used. Such a storage consists of a packed bed of ceramic material that acts as storage mass. During charging, hot air is passing from the top of the storage vessel through channels in the ceramic bed, heating the material by convective heat transfer. With increasing charge level, a larger fraction of the bed inventory is heated to the upper temperature, with the temperature front moving from the top to the bottom. When discharging, cold air is entering the storage from the bottom, and is heated while passing through the packed bed. Thus the temperature front is moving from bottom to top during discharge. A storage system of this type is used in the solar tower demonstration system in Jülich, Germany.

2.6 HYBRIDIZATION

Short Summary:
* Hybridization ensures availability of capacity independent from solar radiation.
* Additional value for grid management.
* Can use fossil or bio-fuels, depending on availability.

An additional unique feature of CSP plants is the optional integration of a burner to provide the heat required for operation of the power block. Using this co-firing option ensures full power availability, even when sun is not shining and storage is emptied (e.g. after some cloudy days). Therefore, the provision of additional grid capacity (backup capacity) with limited operation hours per year can be avoided. This is especially important in regions where limited backup capacity is available in the grid, which is usually the case in markets with increasing power demand.

As the CSP plant already includes a complete thermal power cycle, only a small additional investment is required for the burner, appropriate heat exchangers and auxiliary equipment. The energy source for the burner depends strongly on local conditions and availability, it can be fossil fuel (natural gas, LPG, Diesel, ..) or bio-fuel.

The amount of co-firing can be designed quite freely, it mainly depends on the grid requirements (value of ensured capacity), plant operation strategy, and legal framework. As an example, the legal framework plaid an important role in the CSP market introduction in Spain, as the Spanish feed-in tariff allowed for up to 15% fossil co-firing.

Another solar-hybrid system configuration is the so-called ISCC (Integrated Solar Combined Cycle) concept. In this concept solar generated steam is introduced into the bottoming cycle of a Combined Cycle plant. This configuration was selected for several commercial power plants (e.g. Kuraymat, Egypt, see Fig. 28), but so far only in combination with Parabolic trough systems. However, when the costs get lower, such a configuration can be also realized with a solar tower system. While the gas turbine section is usually run independent of the solar energy, the additional power from the sun is used to boost the power output of the steam cycle, i. e. during sunshine hours the total power output is increased.

One severe restriction of the ISCC concept is the limited annual solar share, which is usually below 10%. For example, in the case of the Kuraymat plant the annual solar share is 4%.
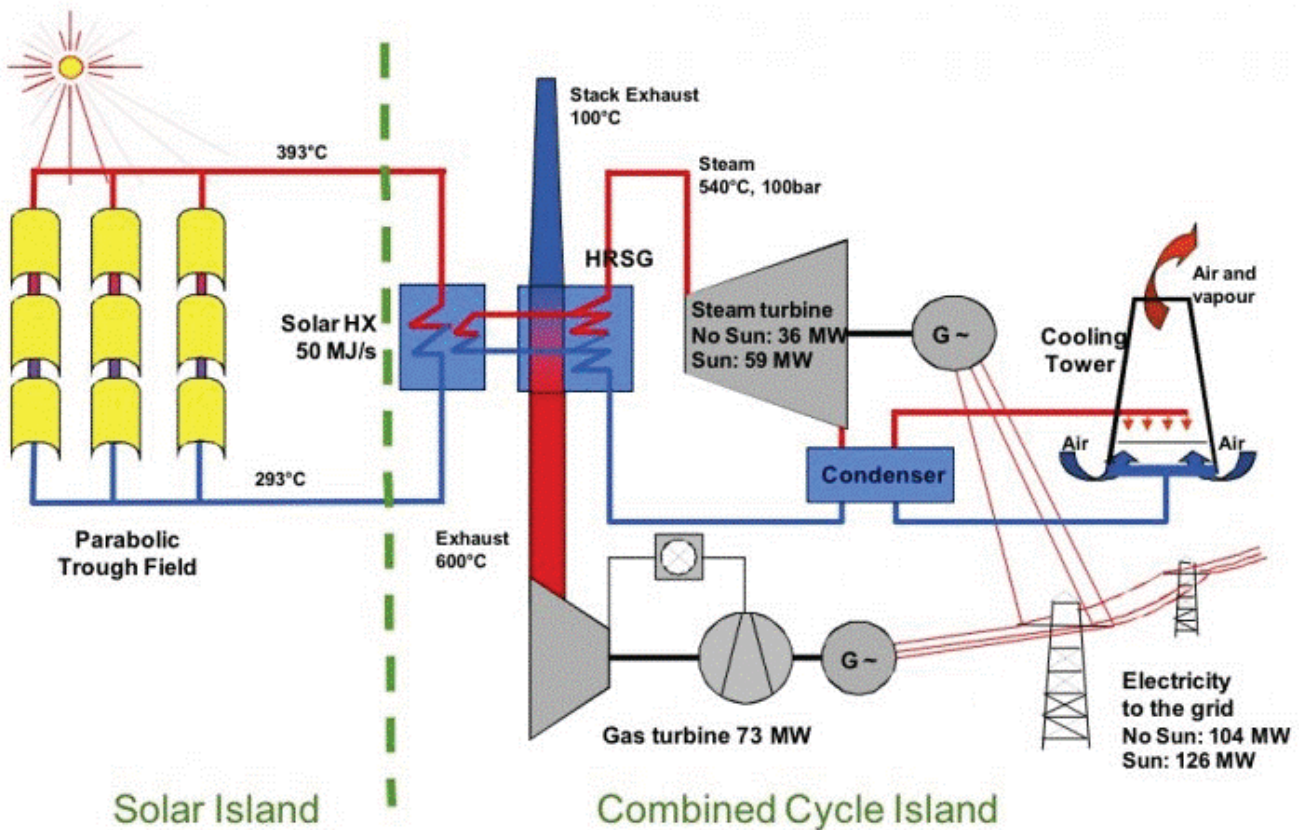
Figure 28: ISCC plant scheme (Kuraymat, Egypt) [25]

2.7 POWER BLOCK

Short Summary:
- The power block of a CSP plant is similar to that of a conventional power plant.
- Current CSP plants use steam cycles that are adapted to the specific conditions of the solar subsystem (temperatures, reheat stages, frequent start-up/shut down cycles, …).
- ISCC concept: Integration of solar-generated steam into the bottoming cycle of a combined cycle plant, with low annual solar share.
- Options exist for advanced power cycles with higher efficiencies.

Electricity generation is the primary objective of CSP plants. Thermal CSP plants produce electricity from thermal energy quite conventionally by thermodynamic and electrochemical conversion. They inherently provide the capability of storing energy in thermal form, if it is not directly converted, or used immediately for heat purposes.

In a CSP plant, electricity is usually generated centrally by one power conversion unit ("power block"), i.e. the functional combination of a generator with a turbine as prime mover. Thermodynamic cycle processes have profound impact on operating domains and generating characteristics of CSP plants, therefore some considerations associated with thermal energy to electricity conversion are of basic interest [53].

Several thermodynamic conversion processes exist, each with distinct operating regimes and characteristics [54]. Of these, two processes have

attained importance in thermal power plant engineering for large installations: The Rankine cycle with water/steam as phase change medium in a closed loop (conventional and superheated steam), and the Brayton cycle with air/gas as working medium in an open loop. For the operating conditions in conventional power plants, thermodynamic conversion technology is mature and the experience broad based. This does not necessarily hold true, however, if such prime movers have to be operated under the non-steady-state, frequently variable input conditions characteristic of CSP [53].

There are other thermodynamic cycles which are also of practical significance for thermal CSP plants. These are the closed-loop Rankine cycle with organic phase-change media (Organic Rankine cycle, ORC), and the closed-loop superheated Brayton cycle with carbon dioxide as working medium (s-CO$_2$).

The Carnot efficiency defines the physical limits for conversion of heat into mechanical work merely as a function of highest to lowest cycle temperature. The conversion quality of thermodynamic cycles achieved in practical settings is expressed in relation to this limit, usually at nominal steady-state operating conditions. Off-nominal operating conditions reduce this relation, sometimes significantly, depending on cycle and converter type, capacity and operation parameters [53]. An overview of possible CSP plant power block conversion efficiencies compared to the theoretical Carnot efficiency is shown in Fig. 29. Of importance for the solar tower technology that is capable of generating high temperatures is in the range between 500 to 1000°C.
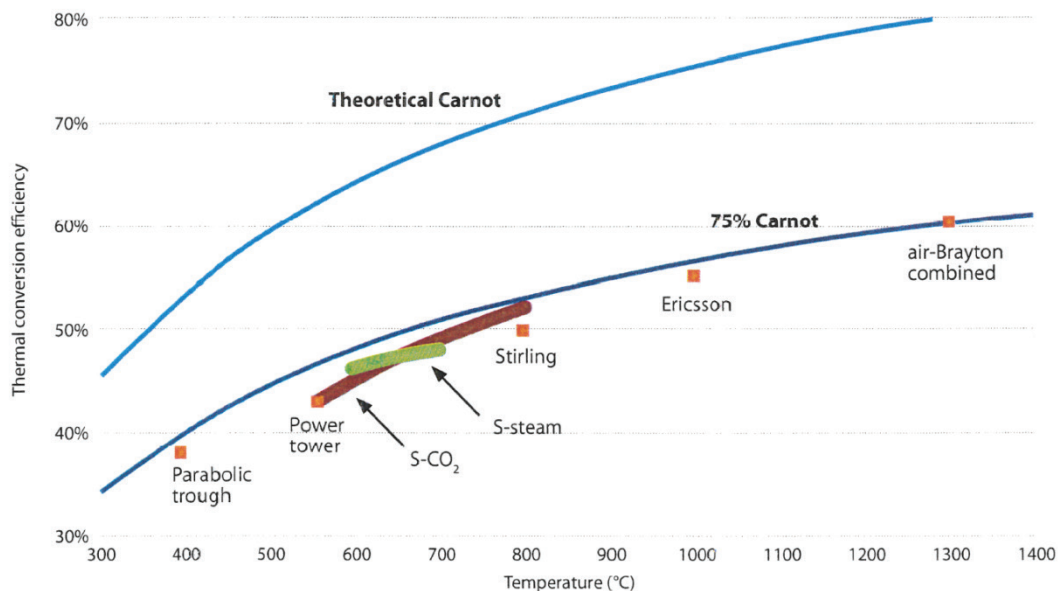
Figure 29: Carnot efficiency of various power cycles [62]

Steam Cycles (Rankine)

The schematic diagram of a simple Rankine cycle is displayed in Fig. 30. The T-s diagram of the corresponding thermodynamic process is also displayed. Feed water (1) is compressed by the feed-water pump (2) and fed to the boiler. In the boiler the feed water is pre-heated, evaporated, and finally superheated. The superheated live steam (3) is expanded in a steam turbine that runs a generator. The expanded wet steam (4) is condensed and fed by the condensate pump to the pre-heating section and the deaerator [55].
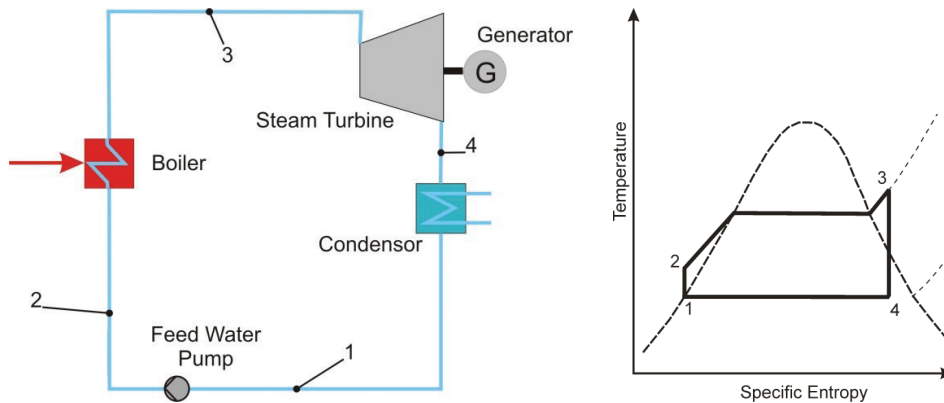
Figure 30: Schematic diagram of a Rankine cycle (left); T-s- diagram (right) [55]

In principle, the Rankine cycle includes the following idealised thermodynamic processes:

1. Isentropic compression (1 » 2)
2. Isobaric heat supply (2 » 3)
3. Isentropic expansion (3 » 4)
4. Isobaric condensation (4 » 1)

Concerning efficiency, in principle, the same rules as for the Carnot cycle apply: The efficiency can be improved by increasing the upper process temperature (T3) and the corresponding pressure (p3), or by reducing the lower process temperature (T4) and the corresponding pressure (p4). In real systems this is realised by increasing the live steam temperature and pressure and reducing the condensation temperature [55], [56].

Thermal stability of the considered working fluid commonly limits the operating temperature of Organic Rankine Cycles (ORC) from below 100°C to 300°C. Regarding CSP plants, ORC cycles can be an option for energy conversion in low temperature parabolic through plants, or as a bottoming cycle in combined cycle power blocks.

Gas Turbine Cycles (Open Brayton) [55]

Fig. 31 displays a schematic diagram of the layout and a T-s diagram of a Brayton cycle. Ambient air (1) is compressed by the compressor. The compressed air (2) is fed to the combustion chamber. In the combustion chamber the air is heated by burning fuel (usually natural gas). The compressed and heated air (3) expands in the turbine (4) that is coupled with an electric generator. The remaining heat is rejected to the atmosphere via a stack. Compared to the Rankine cycle, the Brayton cycle usually is an open cycle, since the flue gas is not returned to the inlet of the compressor.
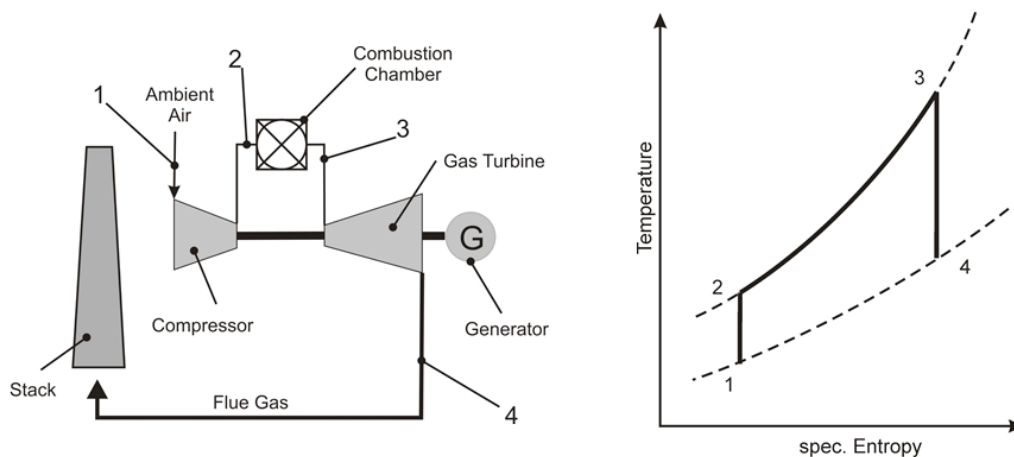
Figure 31: Schematic diagrams of a Brayton cycle (left) and corresponding T-s diagram (right) [55]

The ideal Brayton cycle has the following thermodynamic process steps:

1. Isentropic compression   (1 » 2)
2. Isobaric heat supply   (2 » 3)
3. Isentropic expansion   (3 » 4)
4. Isobaric heat rejection   (4 » 1)

The efficiency of the Brayton cycle is again increased, if the upper process temperature (T2) is increased and/or the lower process temperature (T4) is decreased. This is equivalent with the increase of the pressure ratio p3/p4.

Combined Cycles [55]

Since the flue gas temperature of modern gas turbines is still high the remaining heat is used to generate steam by passing the flue gas through a heat recovery steam generator (HRSG). The schematic diagram and the corresponding T-s diagram of this combined cycle are displayed in Fig. 32. Usually, the two cycles are called topping cycle (Brayton) and bottoming cycle (Rankine).

According to the usual definition of the efficiency as the ratio of useful power to the heat input, the efficiency of the combined cycle can be written as:

$$\eta = \frac{\dot{W}_{GT} + \dot{W}_{ST}}{\dot{Q}_{GT}} = \eta_{GT} + \eta_{ST} \cdot \left(1 - \eta_{GT}\right)$$

$\dot{W}_{GT}$ is the power of the gas turbine and $\dot{W}_{ST}$ the power of the steam turbine. $\dot{Q}_{GT}$ is the heat input into the combustion chamber. Accordingly, the efficiency is always higher than the one of the Brayton cycle. Modern combined cycles reach thermal efficiencies of almost 60% which is the highest efficiency in conventional power plants.
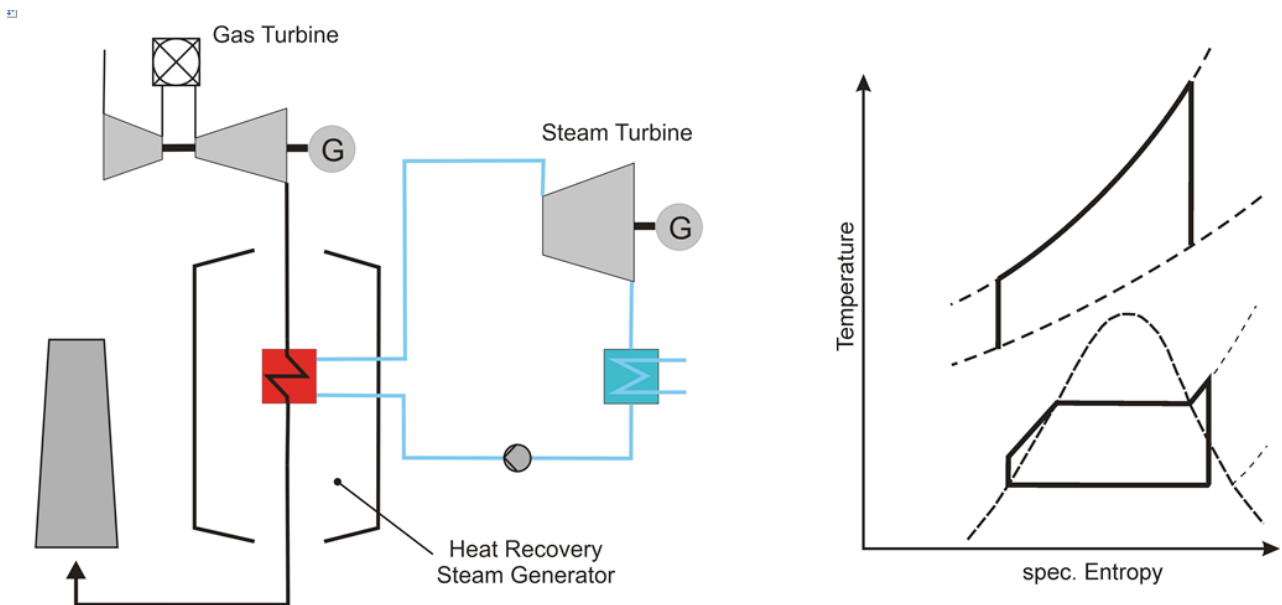
Figure 32: Schematic diagram of a combined cycle (left); corresponding T-s diagram (right) [55]

Such combined cycle systems offer several options for the integration of solar heat:

- Integration of solar-generated steam into the bottoming cycle: this can be enabled either by operating the gas turbine at reduced load whenever solar heat is available, or by oversizing the steam turbine to accept additional steam when solar heat is available. This concept is called ISCCS (Integrated Solar Combined Cycle System).
- Integration of solar heat into the gas turbine: the compressed air can be heated by solar energy, thus reducing the fuel required to heat the air up to turbine inlet temperature. This concept is called "solar gas turbine system".

s-CO$_2$ (Closed Brayton)

Superheated carbon dioxide cycles (s-CO$_2$) have not been considered in solar plants until recently, and research related to its origins from the nuclear power plant industry. In contrast to open-loop Brayton cycles, superheated CO$_2$ cycles rely on a closed-loop Brayton cycle with recompression of the supercritical fluid near its critical point. The operation remains supercritical throughout the entire cycle, and recompression near the critical point takes advantage of the fluid's relatively high density to minimize the compressor power [57].

A single-phase process using s-CO$_2$ as both heat transfer fluid (HTF) and thermal power cycle fluid offers the potential of equivalent or higher cycle efficiency versus supercritical or superheated steam cycles. Such a system offers a simplified power system configuration and would be operated at temperatures relevant for CSP applications. However, the high pressure required for s-CO$_2$ bears a challenge for secure and cost-effective piping [58].

3 LAYOUT PROCESS

This chapter describes the basic procedure for the layout of a solar tower plant, including some examples for layout tools. Factors influencing the layout are discussed.

3.1 INFLUENCING FACTORS ON CRS LAYOUT

Unlike the other concentrating technologies (Parabolic trough, Linear Fresnel, parabolic dish) in central receiver systems concentrator and receiver are not connected by a rigid mechanical construction to form an industrially repeatable unity. Instead, the concentrator consists of numerous independent units (the heliostats) and the receiver is placed on top of a tower, a tall building some distance away. That is why, in contrast to the other CSP technologies, the optical layout (i.e. the positioning of receiver and concentrator relative to each other) is influenced by the local conditions (e.g. the topology of the terrain) and influences itself the plant design and the construction process.

A central receiver system is a point focusing system where the concentrator, ideally a parabolic dish, is fragmentized and the pieces are put on the ground. Consequently, the concentrator cannot be moved as a whole anymore to track the sun's motion. Instead, the concentrator fragments (i.e. the heliostats) are moved independently while they remain fixed on their position on the ground. Obviously, the power reflected to the receiver is not constant but changes from moment to moment as the heliostats track the sun: Mirrors perform an off-axis-reflection where the effective reflector area changes permanently, and heliostats can shadow each other or block reflected light. Moreover, these effects are influenced not only by the current position of the sun but also be the position of each mirror in relation to the receiver and to (most of) the other mirrors.

As a result, the layout process for a solar tower system differs significantly from that of the other technologies. It is the task of the layout process to define the number and position of the heliostats and the size and position of the receiver on top of the tower. The boundary conditions that make this task challenging are obvious: First, the receiver size (more precisely: the size of the receiver aperture) has a strong influence on its thermal losses, so that it is prohibitive to just increase the receiver size to collect all the reflected light. Second, the capital cost of the heliostats does not allow to simply install as many mirrors as needed to provide the demand heat rate. Hence, detailed calculations are necessary to fulfill that task, which are to some extent unique for each plant.

Therefore, the loss mechanisms that occur during concentration have to be analyzed in detail:
- Shadowing of mirror areas by neighboring heliostats
- Reflection loss due to imperfect specular reflectivity
- Cosine loss, i.e. the reduced effective mirror size due to off-axis-reflection
- Blocking of reflected light by neighboring heliostats
- Attenuation of reflected light between heliostat and receiver due to absorption and scattering processes in the atmosphere
- Reflected light reaching the receiver plane but not entering the aperture ("spillage") due to imperfect alignment of the heliostat or oversized reflection image

The latter effect (oversized reflection image) occurs for the heliostats with the largest distance to the receiver. The reason is, because due to the finite size of the sun's disk even with ideally concentrating mirrors the sunlight cannot be concentrated to a single point but to a focal spot of about 0.5 degree of angular extension. Imperfections of real mirrors enlarge this beam divergence and as a result the image size increases with increasing distance of the heliostat to the receiver.

Now, the main effects can be identified that are

competing during the layout of the heliostat field:

On one hand, losses due to shadowing and blocking among neighboring heliostats can be best reduced by increasing the distance between heliostats, i.e. by decreasing the field density.

On the other hand, the losses related to attenuation and spillage increase directly with the distance from the tower, hence they rise for low field densities.

3.2 TOOLS FOR SOLAR TOWER SYSTEM LAYOUT

Although the above mentioned effects can be calculated with sufficient accuracy, it is impossible to solve the layout task analytically. Each heliostat has two degrees of freedom for its position. Accordingly, for a field with just 1000 heliostats the dimension of the space of possible solutions is $= 2^{1000} > 10^{300}$!!

Obviously, problems of this complexity can only be accessed by model based simulation and related optimization methods. This is the reason, why the development of solar tower systems was accompanied by the development of computer based simulation programs since the early seventies. These computer codes use mathematical models to estimate the performance of a solar tower plant (heliostat field + receiver) for a single time point or a period of time. System improvement is done by heuristic methods, while the complexity of the field layout problem is mostly reduced by introducing some kind of regular pattern for the heliostat positions. Some of the most important codes are briefly described in the following sections:

University of Houston Code (UHC)

This code was developed in the mid-eighties. It is based on the analytical description of the reflected image by mathematical convolution and solved by a two-dimensional expansion with Hermite polynoms (this analytical solution method was in the early days of computer technology the faster way compared to the alternative Monte-Carlo-Simulation) [29]. The UHC was originally a suite of FORTRAN programs for the purpose of layout and optimization of heliostat field and receiver of large solar tower systems. To save computation time the heliostats are assumed to be positioned in a regular pattern and the heliostat field is divided into cells, i.e. regions of uniform heliostat density or fixed number of heliostats [30]. Cosine, blocking and shadowing are calculated for one representative per cell. Including thermal receiver performance and a detailed cost model allows optimization on cost/performance criteria on an annual basis. A subsequently applied algorithm defines individual heliostat positions from the optimized cell densities. The code was used for the Solar One and Solar Two technology programs of SANDIA in the USA. Today, a new commercial development called TIESOL is based on the UHC.

DELSOL

The DELSOL code was developed at SANDIA for the purpose of performance and design calculations for central receiver systems, first released in 1978 [28]). Due to its calculation speed it ought to be especially useful for layout, optimization and design studies. The optical model is also based on the analytical Hermite polynomial expansion, which was improved at SANDIA. The heliostats are arranged in a radial staggered pattern and the field is subdivided into zones similar to the cells in UHC. The local density of the heliostats in the zones is calculated per default from curve fits to optimized field layouts from the UHC, with a correction factor dependent on tower height. The local field densities can be varied around these default values during optimization. Table 8 shows the parameters varied and kept fixed during an optimization run to describe the philosophy of the layout optimization. Cost models allow system optimization for minimum LCOE.

parameters varied during an optimization run	parameters kept constant during one optimization run
• design point power level • tower height • receiver dimensions • tower location inside constrained land • field boundaries • heliostat spacings (i.e. field density) • storage capacity (for given solar multiple)	• site (location, ambient conditions) • field (pattern type, min and max boundaries) • heliostat (type, size, optical quality) • receiver (type, orientation, ratio of dimensions) • solar multiple

Table 8: Options for layout optimization in DELSOL
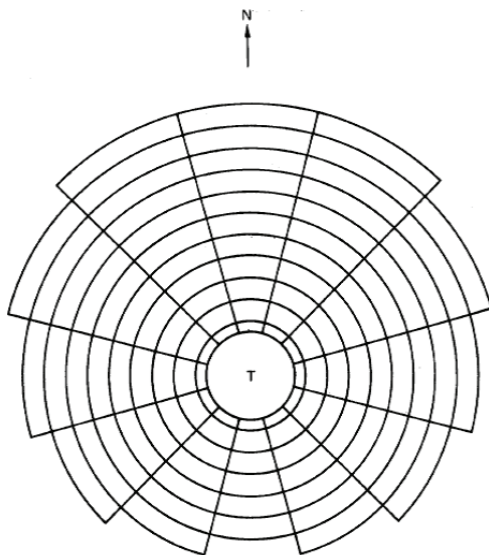
Figure 33: Subdivision of heliostat field into zones in DELSOL [28]

HFLCAL

The program HFLCAL (Heliostat Field Layout Calculations) [21] was generated during the German-Spanish project GAST, a technology program to develop a gas cooled solar tower system. This code is based on the very simple assumption that the flux image from each heliostat can be approximated by a single circular symmetric normal distribution (a so-called "Gaussian"-distribution). The effects of the sun's brightness distribution, mirror imperfections, tracking and astigmatism errors are incorporated into this model leading to a certain image size. This simple approach enables to calculate the instantaneous power provided by a field of thousands of heliostats within very short time (<< 1sec). This allows to analyze a set of representative time points (usually ~100) to estimate the annual performance. Herein, the blocking and shadowing calculations are done analytically for each single heliostat assuming rectangular shape mirrors. This gives the program a great flexibility regarding the field layout patterns: any heliostat arrangement can be analyzed (and if it is described by parameters it can even be optimized). The procedure of layout and optimization therefore differs significantly from the UHC/DELSOL way and is depicted in Fig. 34.
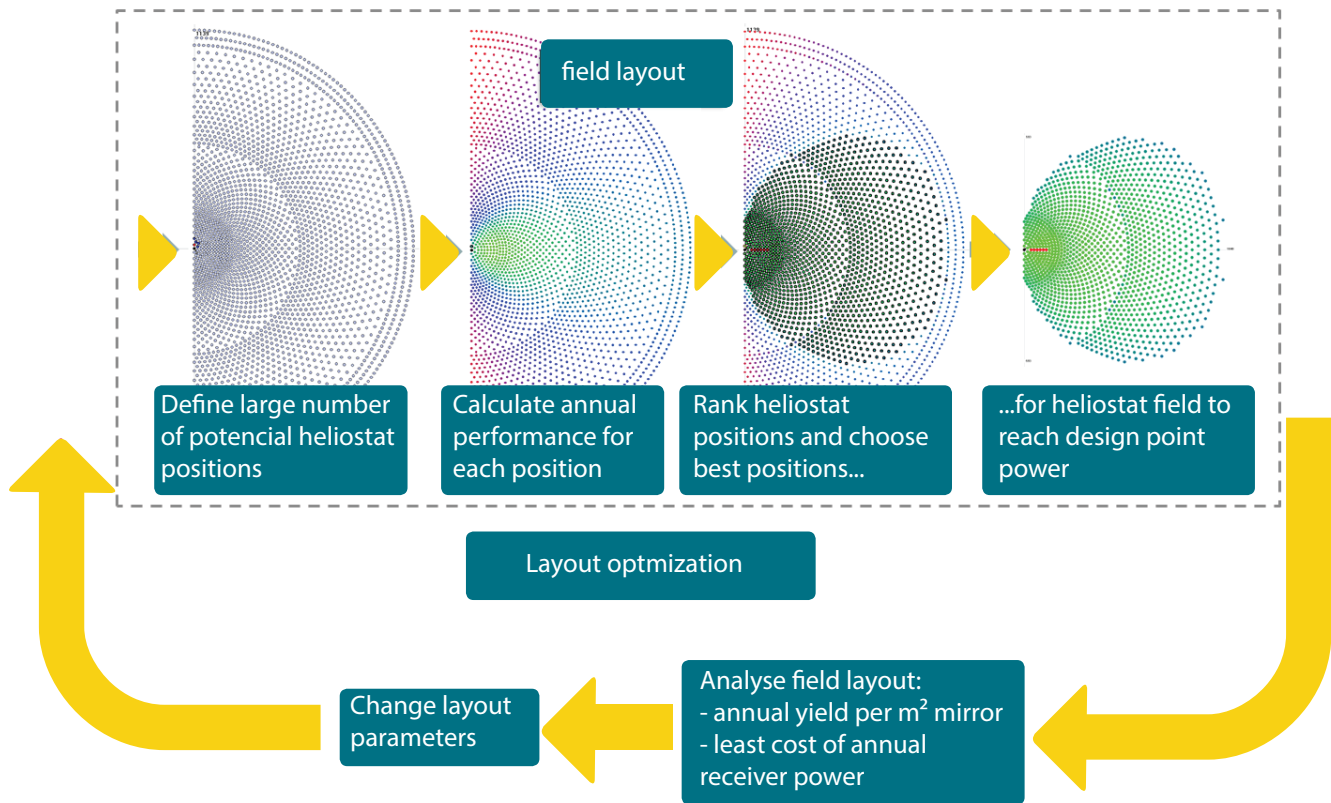
Figure 34: Schematic of field layout and optimization procedure in HFLCAL

parameters varied during an optimization run	parameters kept constant during one optimization run
• heliostat positions (via parameterized pattern) • tower height • receiver size, orientation, ratio of dimensions	• site (location, ambient conditions) • tower location inside constrained land • heliostat (type, size*, optical quality) • receiver (type, geometry) • design point power level (* can also be varied; normally not applied)

Table 9: Options for layout optimization with HFLCAL

3.3 BASIC TENDENCIES OF CRS LAYOUT

The layout of CRS plants is influenced by many technical, ambient, commercial and other parameters as pointed out in the previous chapters. Therefore, a CRS layout is always individual for a specific project. Nevertheless, some general tendencies can be identified .

Heliostats standing north of the tower reflect the sun with a smaller incidence angle compared to those standing south of the tower, which leads to lower cosine losses (Fig. 35). Therefore, heliostat fields are either pure north fields (for flat or cavity receivers facing one direction) or surround fields with an emphasis on the north side.

Accordingly, north fields have a higher annual performance off the equator with a peak at about 30°N, while surround field have the best performance on the equator (see Fig. 36). Both show decreasing performance for higher latitudes >40° because the effect of blocking and shadowing starts to prevail.

Figure 35: Geometric conditions of heliostats standing on both sides of the tower
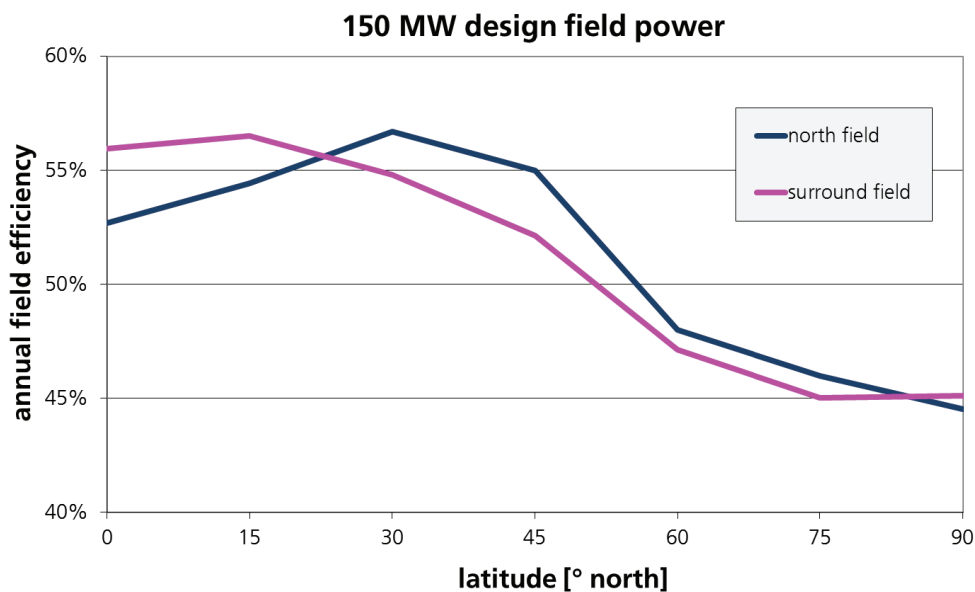
Figure 36: Field efficiency as a function of latitude

When the aperture angle of a cylindrical receiver was a free parameter the field would start to be build up from the north side and fill positions to the east, west and south of the tower with increasing power level (Fig. 33). The trend to build up a surround field is more emphasized at locations closer to the equator. The field efficiency decreases generally with increasing field size (i.e. field power level).

The reason is that more heliostats are standing on less effective positions: either at the south or at the north with larger distance from the tower. In the first case the cosine error prevails and in the latter case blocking, shadowing and spillage losses increase. The decrease of field efficiency with increasing power level is stronger for higher latitudes (Fig. 34).
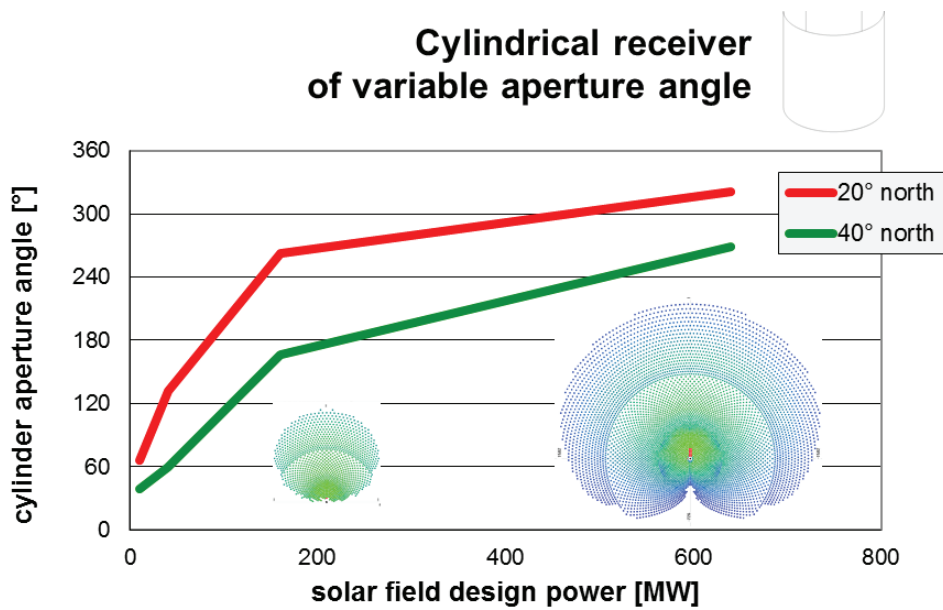
Figure 37: Field shape as a function of power level.
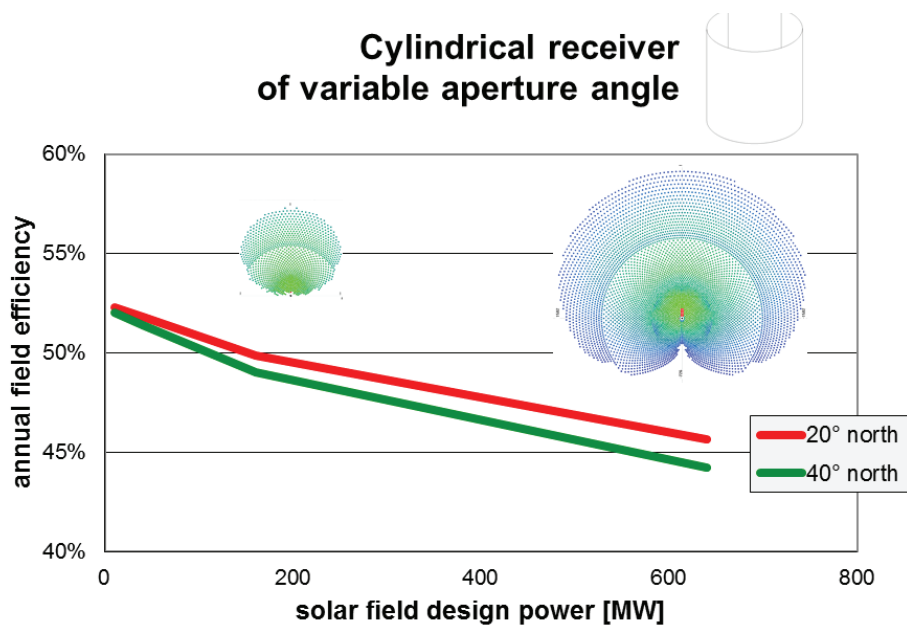
Figure 38: Field efficiency as a function of power level

4 PLANT CONTROL

This chapter gives an overview over the operation and control of a solar tower plant, as well as on methods to improve performance.

4.1 DEFINITION OF CONTROL TASK

A CSP tower plant usually consists of the collector system, the intermediate heat transfer fluid (HTF) cycle and the power block itself, usually a steam turbine cycle. A thermal storage is installed in the heat transfer cycle to decouple heat input and heat demand to a certain extent. Accordingly, the control task can be structured in a similar manner: The objective of the power block control is to deliver the desired electric output. This defines the heat demand to the HTF cycle. The receiver control regulates the HTF mass flow through the receiver. The control criterion usually is a fixed HTF receiver outlet temperature. The solar field control manipulates the heliostat's movements so that the solar radiation is concentrated to the receiver aperture at each moment. As the energy source to the system, the solar irradiation, cannot simply be varied like the fuel of a fossil plant control of solar power plants is a challenging task. Due to the variable nature of the solar source CSP plants are dynamic processes that are operated outside their design conditions most of the time. The thermal storage "buffers" the fluctuating heat input of the supply side and enables a dispatchable power production.

4.2 HELIOSTAT FIELD CONTROL

The motion of the heliostat drives to reflect the solar radiation to the desired aim point on the receiver aperture is usually controlled by an open loop control strategy. The central control unit calculates the current position of the sun from the geographical coordinates of the plant and the time. From the known position of the heliostat and the aim point on the receiver aperture the desired direction of the heliostat normal is calculated. This determines the heliostat orientation in two axes, usually azimuth and elevation. The respective drives are moved to the desired value, which is controlled by encoders on the axes. No direct check is performed to verify that the heliostats reflected image is directed to the desired aim point.

Several effects lead to deviations of the real to the desired aim point:
• Imperfections of the solar position algorithm
• Imprecise geographical coordinates and directions
• Errors in aim point coordinates
• Errors in heliostat positions, geometrical dimensions and directions
• Heliostat drive tolerances and backlash
• Defective encoder signals; finite encoder resolution
• Heliostat structural deformation due to external forces like gravity or wind loads

Typical tracking errors due to these error sources are in the order of magnitude of 1-2 mrad [27], which would be unacceptably high. Therefore, a repeated off-set correction is performed, where a heliostat is directed to a reflecting target below the receiver. A camera observes the deviation of the image on the target from the desired aim point and a corrective motion of the drives is calculated and performed. This is repeated for each heliostat (one after the other) and can be conducted during operation (Fig. 39). The measured deviations from the off-set correction can be used to calibrate an error model that describes the systematic error sources. Like this, the tracking errors can be reduced to about 0.5 mrad after thorough calibration [26]. Closed loop tracking control using CCD cameras close to the receiver is described in literature but not yet widely used [27].
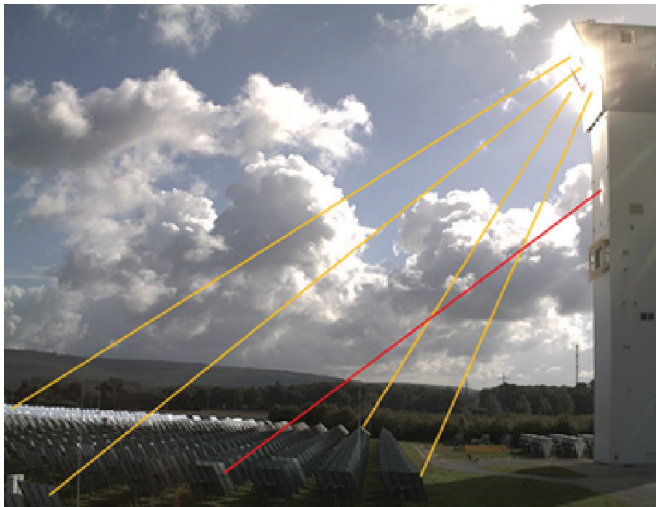
Figure 39: Offset correction at Jülich Solar Tower Plant

4.3 AIM POINT DISTRIBUTION

Assuring, that a heliostat is aiming to its desired aim point does not solve the problem, where the desired aim point should be. Clearly, from a pure energetic point of view aiming at the center of the receiver aperture would minimize the spillage losses. But material constraints regarding maximum temperature and maximum heat load on the receiver surface necessitate spreading the focal spots over the entire aperture.

To reduce the degree of freedom, usually a small number of aim points is defined manually on the aperture and heliostats are assigned to these aim points according to their image size (which corresponds more or less with their slant range): heliostats standing in large distance from the target producing large images are assigned to central aim points (i.e. large distance from aperture edges); heliostats standing closer to the target producing smaller images are assigned to outer aim points (i.e. closer to aperture edges). Heliostats are often assigned in groups of neighboring heliostats and assignment is usually done manually by the operator. Changing of the assignment during the day can be necessary as the heliostats' images change in size and shape according to the solar position.

Due to tracking uncertainties and changing ambient or operational conditions it is not unlikely that the receiver reaches an upper temperature limit somewhere on its surface during a normal operation day. There are usually three options then for the operator or control system to react:
- shifting of one or more aim points (including the assigned heliostats)
- reassignment of single heliostats to another aim point
- defocussing of single heliostats or entire groups of heliostats

Which of these options is chosen depends on the receiver technology, the heliostat type and size and the overall operational control strategy.

These interventions can be done manually by the operators, but they are very time-consuming and tend to be risky. Therefore, several automated systems are described in literature:

In [31] the authors report the automated aim point control developed for the TSA wire mesh volumetric air receiver with six predefined aim points. It was based on a set of thermocouple-measurements inside the receiver during operation and could perform either heliostat adjustment (change of a heliostat from one aim point to another) or aim point adjustment (displacement of aim point).

The aim point control for Solar Two molten salt plant is described in [32]. In the design phase, the heliostats' aim points were spread across the cylinder height according to their beam radius. The allowable flux density was calculated depending on the local salt flow rate and temperature. For receiver protection purposes a model based automatic system, called Dynamic Aim Point Processing System (DAPS) is described. When the allowed flux density is exceeded, the system identifies the heliostat producing the highest flux density at the affected location on the receiver and subtracts its image from the absorbed flux. This procedure

is repeated until the local flux peak is evened out. Then the identified heliostats are defocused.

Recently, a simulation based system has been reported that allows to optimize the distribution of aim points on the target to maximize the receiver power output [33]. A high precision modelling of the heliostat's images is performed based on deflectometry measurement of the mirror surface. The heuristic ant-colony algorithm is applied to find the optimal assignment of heliostats to a distinct number of aim points. The objective of this development is an automated prediction system that is able to deliver the best aim point assignment for a near time horizon (e.g. 15min – 60min) based on actual operation and ambient conditions.

4.4 AUTOMATED OPERATION

Many operation and control actions are still done manually or semi-automatically but the objective is fully automatic operation with human surveillance only. Clearly, due to the complexity of the technical system, model based control strategies are in focus.

In [34] the authors report the development of an operation assistance system. This model based simulation and control system is planned to be established in four steps:
- the prediction mode is delivering a model based forecast of the future state of the power plant
- the maneuver mode enables the plant operator to find out about the consequences of his planned system changes
- the proposal mode makes suggestions to the operator about how he should change system parameters to drive the plant in an optimized way; this is the actual operation assistance system
- the final step is the model predictive control, where the system evaluates the best operation condition and automatically sets system parameters accordingly

5 OVERVIEW ON COMMERCIAL SOLAR TOWER PLANTS

This overview is focusing on the commercial solar tower plants, both in operation as well as under construction and planning. In addition, solar tower demonstration systems and solar tower test facilities are briefly described.

5.1 COMMERCIAL SOLAR TOWER PLANTS IN OPERATION

So far only a few solar tower plants are operated on a commercial basis for day-by-day power production. These commercial solar tower plants are described in the order of commissioning.

PS10 / PS20
Sources: [25][36]

solar resource (TMY)	2012 kWh/m²a
plant	PS10 / PS20
developer	Abengoa Solar
location	Sanlúcar la Mayor, near Seville, Spain
electric power rating	11 / 20 MW
net annual power production	24.3 GWh/a / 48.6 GWh/a
capacity factor	24.3% / 27.4%
land area	0.55 km² / 0.8 km²
heliostat field	75 000 / 150 000 m²
number of heliostats	624 / 1255
heliostat area	120 m2
heliostat type	T-type
reflector material	backsilvered mirror, low iron glass
drives	dual worm gear, electric
tower	
type	concrete
height	115 m / 165 m
receiver	
type	cavity
heat transfer fluid	water / steam
thermal power (DP)	55 MWt / 110 MWt
receiver inlet / outlet temperature	- / 250°C
receiver efficiency (DP)	92%

average flux density (DP)	500 kW/m²
storage	
type	Ruth (pressurized water / steam)
storage capacity	1h (15MWh) / 1h (part load)
power cycle	
type	saturated steam cycle, wet cooling
cycle efficiency (DP)	30.75%
begin of construction period	2004 / 2006
start of operation	2007 / 2009

Figure 40: Solar tower plants PS10 and PS20 (Spain)

Other remarks:
- Mirror cleaning: Truck-mounted spray and brush units

Figure 41: Abengoa truck with mirror cleaning equipment [38]

Gemasolar

Sources: [25][40][41][42][43][44]

solar resource (TMY)	2172 kWh/m²a
plant	Gemasolar
developer	Torresol
location	Fuentes de Andalucia, near Seville, Spain
electric power rating	19.9 MW
net annual power production	110 GWh/a
capacity factor	74%
land area	1.95 km²
heliostat field	304 750 m²
number of heliostats	2650
heliostat area	115 m²
heliostat type	T-type
reflector material	backsilvered mirror, low iron glass
drives	dual worm gear, electric
tower	
type	concrete
height	140 m
receiver	
type	external, cylindrical
heat transfer fluid	molten salt ("solar salt")
thermal power (DP)	120 MWt
receiver inlet / outlet temperature	290°C / 565°C
receiver efficiency (DP)	~88%
average flux density (DP)	~ 540kW/m²
storage	
type	two-tank molten salt, direct
storage capacity	15 h
power cycle	
type	superheated steam cycle, wet cooling
cycle efficiency (DP)	40%
begin of construction period	2009
start of operation	2011

Figure 42: Solar tower plant Gemasolar (Spain)

Figure 43: Sener cleaning truck (left), cleaning robot (right)

Remarks:
- Gemasolar was producing power around the clock for 36 consecutive days in 2013
- Torresol is owned by MASDAR (40%) and Sener (60%)

Sierra SunTower
Sources: [25] [46]

solar resource (TMY)	2 629 kWh/m²a
plant	Sierra SunTower
developer	eSolar
location	Lancaster/CA (USA)
electric power rating	5 MW
net annual power production	4.27 GWh/a (expected)
capacity factor	9.7%
land area	0.08 km²
heliostat field	27 670 m²
number of heliostats	24 360

heliostat area	1.14 m²
heliostat type	T-type
reflector material	backsilvered mirror, low iron glass
drives	electric motors with gears
tower	2 towers
type	steel tube (wind turbine tower)
height	55 m
receiver	
type	1 dual-cavity, 1 external
heat transfer fluid	water/steam
thermal power (DP)	- MWt
receiver inlet / outlet temperature	218°C / 440°C
receiver efficiency (DP)	89%
average flux density (DP)	- kW/m²
storage	
type	none
storage capacity	-
power cycle	
type	superheated steam cycle, wet cooling
cycle efficiency (DP)	21%
begin of construction period	2008
start of operation	2009

Figure 44: Solar tower plant Sierra SunTower (USA)

Ivanpah Solar Electric Generating System (ISEGS)
Sources: [25]

solar resource (TMY)	2717 kWh/m²a
plant	ISEGS
developer	Brightsource
location	Ivanpah Dry Lake (CA, USA)
electric power rating	377 MW
net annual power production	1 079 232 GWh/a
capacity factor	32.7%
land area	14.2 km²
heliostat field	2 600 000 m²
number of heliostats	173 500
heliostat area	15 m²
heliostat type	T-type
reflector material	backsilvered mirror, low iron glass
drives	electric; worm gear (azimuth), linear actuator (elevation)
tower	3 towers
type	steel framework
height	140 m
receiver	
type	external tube receiver
heat transfer fluid	water/steam
thermal power (DP)	- MWt
receiver inlet / outlet temperature	250°C / 550°C
receiver efficiency (DP)	-
average flux density (DP)	- kW/m²
storage	none
type	-
storage capacity	-
power cycle	
type	superheated steam cycle, dry cooling
cycle efficiency (DP)	28.7%
begin of construction period	2010
start of operation	2014

Figure 45: Solar tower plant ISEGS (Ivanpah, CA/USA)

Remark: Brightsource has built another solar tower plant in Coalinga (CA, USA) with a thermal receiver design power of 29 MWth. This solar tower system is used for thermal enhanced oil recovery (EOR) and does not include a power block. The heliostat field consists of 3822 heliostats, the project was delivered to the client Chevron in October 2011.

5.2 SOLAR TOWER PLANTS UNDER CONSTRUCTION

Crescent Dunes
Sources: [25]; CSP Project Fact Sheet 09/2013, by SolarReserve

solar resource (TMY)	2685 kWh/m²a
plant	Crescent Dunes
developer	SolarReserve
location	Tonopah (NV, USA)
electric power rating	110 MW
net annual power production	485 GWh/a
capacity factor	50%
land area	6.5 km²
heliostat field	1 194 800 m²
number of heliostats	10300
heliostat area	116m²

heliostat type	T-type
reflector material	3mm backsilvered mirror, low iron glass, stamped steel sheet backing
drives	cycloidal gearbox drive, linear actuator for elevation
tower	
type	concrete, slip formed
height	198 m
receiver	
type	external tube receiver
heat transfer fluid	molten salt
thermal power (DP)	565 MWt
receiver inlet / outlet temperature	288°C / 565°C
receiver efficiency (DP)	90% (estimated)
average flux density (DP)	- kW/m²
storage	
type	two-tank direct, efficiency: 99%
storage capacity	10 h
power cycle	
type	steam cycle, hybrid wet/dry cooling
cycle efficiency (DP)	40% (estimated)
begin of construction period	2011
start of operation	expected 2014

Figure 46: Solar tower plant Crescent Dunes (Tonopah/USA)

Khi Solar One

Sources: [25]

solar resource (TMY)	- kWh/m²a
plant	Khi Solar One
developer	Abengoa Solar
location	Upington (South Africa)
electric power rating	50 MW
net annual power production	180 GWh/a
capacity factor	41%
land area	1.4 km²
heliostat field	576 800 m²
number of heliostats	4 120
heliostat area	140 m²
heliostat type	T-type
reflector material	thin glass mirrors on sandwich facets
drives	hydraulic
tower	
type	concrete
height	205 m
receiver	
type	tube receiver
heat transfer fluid	water/steam
thermal power (DP)	MWt
receiver inlet / outlet temperature	- / 530°C
receiver efficiency (DP)	-
average flux density (DP)	- kW/m²
storage	
type	saturated steam
storage capacity	2 h
power cycle	
type	superheated steam cycle, dry cooling
cycle efficiency (DP)	-
begin of construction period	2012
start of operation	expected 2014
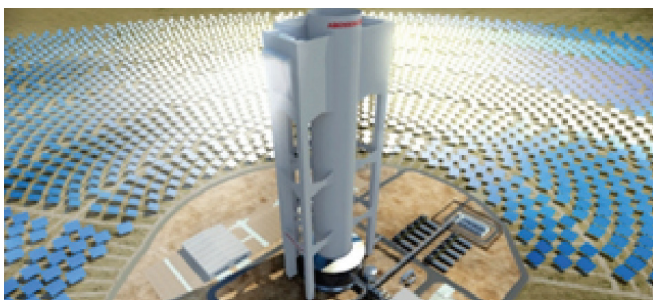
Figure 47: Khi Solar One (artist view)

SUPCON

Sources: [25]

solar resource (TMY)	- kWh/m²a
plant	Supcon solar project
developer	Supcon Solar
location	Delingha/China
electric power rating	50 MW
net annual power production	120 GWh/a (expected)
capacity factor	27%
land area	3.3 km²
heliostat field	434 880 m²
number of heliostats	217 440
heliostat area	2.0 m²
heliostat type	-
reflector material	-
drives	-
tower	multitower: 10 towers
type	steel framework
height	80 m
receiver	
type	
heat transfer fluid	
thermal power (DP)	MWt
receiver inlet / outlet temperature	°C / °C
receiver efficiency (DP)	88%
average flux density (DP)	kW/m²
storage	
type	molten salt
storage capacity	-
power cycle	
type	steam cycle
cycle efficiency (DP)	40%
begin of construction period	2010
start of operation	1st tower in operation

Figure 48: Solar tower plant Supcon (Delingha/China) [51]

5.3 ANNOUNCED SOLAR TOWER PLANTS

A few other solar tower plants were announced and are in different stages of the planning / permission process. These plants are:

• Ouarzazate 3 (NOOR III): the plant is expected to be a 100 MW power tower with up to 3h energy storage; tender process ongoing, with 4 pre-qualified consortia

• Palen: Riverside County, CA/USA, 500 MW nominal in two solar tower units; expected construction start date: 2013/2014; developer: Brightsource Energy

• Chile, Atacama desert: 110 MW solar plant using tower technology with 17.5h of thermal energy storage, with molten salt technology; developer: Abengoa

5.4 SOLAR TOWER DEMONSTRATION PLANTS

Solar Tower Jülich
Sources: [25][47]

solar resource (TMY)	902 kWh/m²a
plant	Solar Tower Jülich
developer	KAM
location	Jülich (Germany)
electric power rating	1.5 MW
net annual power production	110 GWh/a
capacity factor	74%
land area	0.8 km²
heliostat field	17 650 m²
number of heliostats	2 153
heliostat area	8.2m²

heliostat type	horizontal 1st axis
reflector material	backsilvered mirror, low iron glass
drives	electric linear actuators
tower	
type	concrete
height	60m
receiver	
type	
heat transfer fluid	external, open volumetric
thermal power (DP)	air
receiver inlet / outlet temperature	- MWt
receiver efficiency (DP)	120°C / 680°C
average flux density (DP)	
storage	- kW/m^2
type	
storage capacity	regenerator, packed bed
power cycle	1.5h
type	
cycle efficiency (DP)	superheated steam cycle, dry cooling
begin of construction period	-
start of operation	2007
	2008

Figure 49: Solar tower plant STJ (Jülich/Germany)

Other demonstration plants:

	SOLUGAS	VAST	Greenway	Dahan	Acme Solar Power 1	Lake Cargelligo
location	Seville (Spain)	Forbes (Australia)	Mersin (Turkey)	Beijing (China)	Bikaner (India)	Lake Cargelligo (Australia)
power	4.5MW	1.2MW	5MWth	1MW	2.5MW	3MW
heliostat number		5 x 700	510	100	14280	620
heliostat size		-		100m²	1.136m²	6.08m²
tower height		27m			46m	
receiver		not disclosed	tube receiver, 550°C 55bar	water/ steam	water / steam 218°C	graphite storage receiver, water / steam 500°C/50bar
storage	hybrid, no storage	foreseen	hybrid, no storage	1h	440°C 40bar	integrated in receiver
start of operation	2012		2013	2012	no storage	2011
remarks		5 units				

Small solar tower system:

AORA
AORA's Tulip system is a modular distributed solar thermal technology that is configured in compact base units. Each module consists of a heliostat field with tower and receiver and a microturbine. The system is solar-hybrid, i. e. it can be operated on sun, on fuel and in mixed mode. The microturbine produces 100kWe and up to 170kW of heat that can be used for heating, cooling (absorption chillers), hot air/water for industrial and domestic processes.

SMILE
Two solar-hybrid gas turbine systems (similar to the AORA system) are planned for erection in Brazil. Both systems will offer 100kWe plus process heat of up to 170kW. These systems will use tube receivers to preheat the combustion air to 800°C. Ground-breaking is foreseen in 2014.

5.5 TEST FACILITIES

There exist a number of solar tower test facilities that were and are used for numerous R&D projects for solar tower system components. These test facilities are located in several countries all over the world:
• PSA: Plataforma Solar de Almería, Spain; two solar tower systems of 2.5 and 5MW thermal power
• CTAER: Located directly beside the PSA; this new test facility uses an innovative heliostat field with the heliostats moving on rails around the tower
• Themis: Targasonne, France; test facility with a heliostat field situated on mountain slope
• SNL: Solar tower test facility with a thermal power level of 5MW
• Solar Tower of Weizmann Institute of Science: Rehovot, Israel; test facility with 3MW
• CSIRO: Newcastle, Australia; two solar tower test systems
• KSU: Riyadh, Saudi-Arabia: this solar test facility has a thermal power of about 200kW and is currently under construction
• HEUREKA: Near Seville, Spain; this Abengoa test facility was used for development of superheated steam and molten salt receivers

6 ECONOMIC PARAMETERS

This chapter gives an overview over the cost situation of solar tower systems. Capital costs (investment in plant components, infrastructure, financing costs) and operation costs are discussed.

6.1 INTRODUCTION

The most common assessment criteria for the economy of CSP plants are the LCOE (Levelized Cost of Electricity) or sometimes also referred as LEC (Levelized Electricity Cost). The LCOE represents the equivalent cost of each unit of electricity generated ($/kWh) during the lifetime of the project taking into account the initial investment (CAPEX), operation and maintenance costs (OPEX) and financing costs associated with interest on any borrowings. It represents the real cost of producing electricity where revenues would equal costs (CAPEX, OPEX and financing costs) excluding tax payments. Therefore, the LCOE is not the selling price that a developer aims at achieving in PPA negotiations, since it does not include tax payments and the expected equity internal rate of return (IRR) expected by the developer. Apart from taking into account financing costs, the LCOE is very much related with the technology itself and is independent of a developer's expected IRR. LCOE is a fixed value which does not escalate over time [62]. The following figure shows a typical LCOE cost breakdown of a solar tower, where the annualized CAPEX include the financing costs and account for over 80%. Unlike conventional power plants, the LCOE of CSP plants is dominated by the initial investment costs. In that sense for a CSP plant the "fuel" (i. e. the equipment to collect the solar energy) for the plant operation is bought at the beginning of the project. Due to the high investment costs a solid project financing is crucial for CSP plants. Confidence of the investors in the selected CSP technology is very important to minimize financing cost, as it results in lower interest rates or acceptance of reduced rates of return.
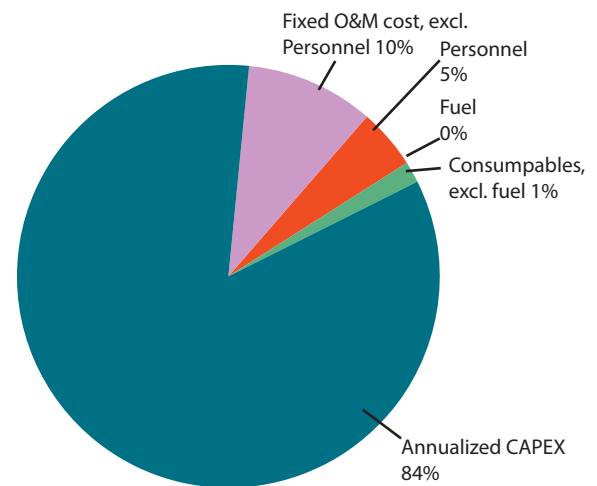
Figure 50: Typical LCOE cost breakdown for 100 MW Solar Tower Plant with 15 hours storage capacity [61]

There are different methods and equations to calculate the LCOE depending on the cost items that are considered and the way the cost data and energy yield are discounted over time. That is why big attention is necessary on the definition of LCOE when comparing the LCOE of different plants and different studies. Not only the technical specifications (like annual DNI, storage size, solar field size, …) may differ, also project specific boundary conditions (like tax incentives, discount model, ..) may differ.

Following a simplified cost model for LCOE calculation is shown, that is according to the model suggested by the International Energy Agency [60]. The objective of this economical calculation is the analysis of the relative differences between systems based on LCOE. Hence, project specific parameters such as taxes, financing concepts, etc. are neglected. Examples for the use of this method can be found in [59].

The IEA-method includes simplifying assumptions:
- 100% financing
- Annuity method
- Operation time = depreciation period
- Taxes are neglected
- Inflation and price increases during the

construction period are neglected
- Inflation and price increases regarding O&M, insurance etc. costs are neglected

Using these assumptions the following correlation is defined:

$$LCOE = \frac{Inv \cdot FCR + O\&M}{E_{el}} \qquad FCR = \frac{i \cdot (1+i)^n}{(1+i)^n -}$$

with

Inv:	Investment costs
FCR:	Fixed charge rate
$O\&M$:	Annual operation, maintenance and insurance cost

E_{el}:	Annual electricity yield
i:	Real debt interest rate
n:	Depreciation period in years
$LCOE$:	Levelized cost of electricity

Keeping in mind that the LCOE method varies from study to study the following table shows a summary for current and expected LCOE data of solar towers [63]. According to this study the LCOE of solar towers ranges in 2011 from 0.16 to 0.28 $/kWh. In 2020 a LCOE from 0.08 to 0.16/kWh is expected. Additionally the table shows a comparison to the Parabolic trough technology, where the authors report slightly higher LCOE than for the solar tower. However, it should be kept in mind that the reliability of the economic figures is better for Parabolic trough technology, due to the higher level of maturity.

CSP type and source	2011		2012		Notes
	Low estimate	High estimate	Low estimate	High estimate	
2010 (USD/kWh)					
Parabolic trough					
IEA, 2010	0.20	0.295	0.10	0.14	Large plant, 10% discount rate
Fichtner, 2010	0.22	0.24			Proposed plant in South Africa. 8% disocunt rate. Lower end is for 100 MW plant with storage
	0.33	0.36			LCOE for India, lower value is for wet-cooled and higher value for dry-cooled
	0.22	0.23			LCOE for Morocco, lower value is for wet-cooled and higher value for dry-cooled
Basedon Kutscher ,et al. 2010	0.22		0.10	0.11	Data for the United States, adjusted to exclude impact of tax credits
Hinkley, et al. 2011	0.21		0.13		Data for a 100 MW plant in Queensland, Australia, 7% discount rate
Solar Tower					
Fichtner, 2010	0.186	0.202			Proposed plant in South Africa. 8% discount rate. Lower end is for 100 MW plant with storage
	0.27	0.26			LCOE for India, lower value is for wet-cooled and higher value for dry-cooled
	0.22	0.23			LCOE for Morocco, lower value is for wet-cooled and higher value for dry-cooled
Kolb, et al. 2010	0.16	0.17	0.08	0.09	Data for the United States, adjusted to exclude impact of tax credits
Hinkley, et al. 2011	0.21		0.16		Data for a 100 MW plant in Queensland, Australia, 7% discount rate

Parabolic trough and solar towers					
A.T. Kearney, 2010	0.23	0.32	0.13	0.16	

Table 10: Estimated LCOE for Parabolic Trough and Solar Tower Projects in 2011 and 2020 [63]

Another common assessment criteria for the economy of CSP plants is the cost per installed capacity ($/kW). It is often used to compare different technologies and projects. However, great attention is needed when comparing the cost per installed capacity since this parameter does not account for the differences in energy yield (or capacity factor), which influence the viability of a project [62]. Although CSP plants with thermal energy storage have higher specific investment costs ($/kW) due to the storage system and the larger solar field, the greater electricity generation will generally result in lower electricity generation cost. Energy storage should therefore be looked at carefully, as it can reduce the cost of electricity generated by the CSP plant and increase electricity production (capacity factors) [63].

6.2 INVESTMENT COST (CAPEX)

Unlike power plants fired by fossil fuels, the LCOE of CSP plants is dominated by the initial investment cost, which accounts for approximately 80% of the total cost. The rest is the cost for operation and maintenance of the plant and for plant insurance [63].

The main investment costs of a solar tower plant are:
• Heliostat field
• Receiver system
• Tower
• Thermal energy storage
• Power block (often including the steam generation system)
• Balance of plant

Solar tower technology is at an early stage of commercial deployment compared with other solar technologies. Over the last few years an increasing amount of data on solar tower costs and the LCOE of this technology have been published. Most of these studies and publications show quite different results, giving the outside reader a misleading perspective of the industry. There is also a significant amount of 'perceived' and 'assumed' knowledge surrounding the cost and performance of solar tower technology that is both inaccurate and confusing. Furthermore, as mentioned, the methodology used to calculate cost and LCOE is usually not well-documented in most of these publications, making it difficult to draw significant and even valid comparisons between sources.

The limited availability of reliable and up-to-date information regarding cost and performance of actual solar tower projects is an important hurdle to the development of this technology. Reality shows that the few developers, EPC companies and component manufacturers that are currently involved in solar tower technology are quite reluctant to discuss and divulge the real cost of their technology; making it difficult to find accurate data about the investment required to set up a solar tower power plant [62].

However, while the conventional part of a solar tower plant (steam generator, steam turbine,…) can be priced quite exactly the individual cost of the solar part show still a high variety, depending on the author and the definition of what is included in the cost. The market prices for the conventional, state of the art components are known and also comparable. For the solar specific components the market is developing at the moment and therefore

exact and reliable prices can only be predicted with a certain inaccuracy. It is clear that just this inaccuracy is the chance for innovations to bring down the investment costs and so the LCOE. However, it is important to use real and reliable data for the solar specific components for an accurate assessment of the solar tower technology. It is common to use specific investment cost of the main components. Some care is needed for those numbers as they do often not consider project specific boundary conditions, economy of scale and mass production.

The following figure shows the typical cost breakdown of a molten salt solar tower with storage. The solar components account for approximately half of the total initial investment costs. From these solar components about 33% are coming from the heliostat field (also named solar field), about 15% from the receiver system and about 2% from the tower cost. This share gives also a good indication where the biggest care about reliable data is needed and where innovations/ cost reductions are especially important to bring down the LCOE.
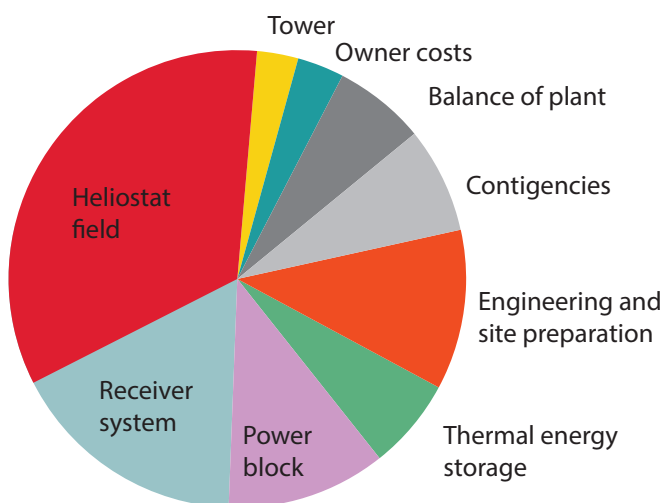

Figure 51: Typical total installed cost breakdown for 100 MW Solar Tower CSP Plant with 15 hours storage capacity [63]

Heliostat investment cost

There are several studies and publications about the price of the heliostat existing. It is most common to specify the heliostat price by specific prices per installed m² reflective area. These installed prices include engineering, fabrication, transport, assembly, cabling, lightning protection and acceptance tests of the heliostat. Some care is needed as some authors define production cost, other define prices. However, the estimated specific installed price is found for example in [64], [65] with 130 to 300$/m², depending on the author and the produced quantity. A SANDIA report [66] estimates the installed price in 2006 of a metal-glass heliostat to be 164$/m2 (for 5000 units/a) and 126 $/m2 given (for 50000 units/a). Fichtner consultants [61] used in their study 2010 a range between 240 and 260$/m2 and CSP Today assumed in their tower report in 2013 about 140$/m2 [62]. In 2011 Sandia National Laboratories defined in their report for the United States Department of Energy (DoE) current baseline cost with 200$/m² and the goal for 2020 is 120$/m² [67]. The current DoE's SunShot target for 2020 is 75$/m² [68].

Tower investment cost

As defined in the previous chapter the tower can be built of different types of structures. Regarding the tower prices there are also several studies and publications available that show still a significant variation in tower cost.

Fig. 52 shows the tower cost against the height of the structure [69]. With these data, for example, a 150m tall tower will cost between 5 or 20 Mio € depending on the author. Some care is needed with the definition of the tower height as some authors include the receiver height and some don't.
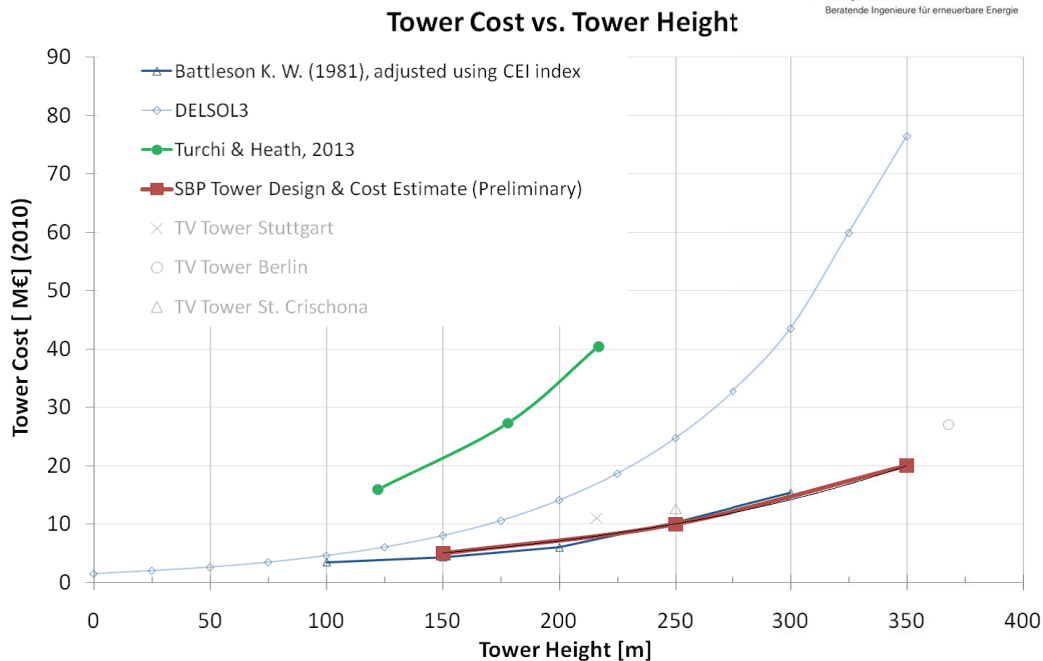
Figure 52: Tower cost against tower height from different authors [69]

Receiver investment cost

As for the other solar specific components for the receiver investment cost there are also different publications showing a significant variation in cost assumptions. The specific cost of the receiver are given in $/kWth or $/m2. Some care is needed for the scope of supply as commonly the receiver system contains more than just the absorber panels. The balance of system like pumps, valves, piping vessels, heat tracing elements (if needed) is normally also included. For a molten salt receiver Sargent & Lundy assumed 2009 for a 120MWth receiver 284$/kWth and for a large receiver (1400MWth) in the long term 70$/kWth [70]. Fichtner consultants [61] used in their study 2010 a range between 200 and 270$/kWth and CSP Today assumed in 2013 about 200$/kWth [62]. In 2011 Sandia National Laboratories defined in their report for the United States Department of Energy (DoE) current baseline cost with 200$/kWth and the goal for 2020 is 170$/kWth [67]. The current DoE's SunShot Target for 2020 is 150$/kWth [68].

6.3 ANNUAL COST OF OPERATION AND MAINTENANCE (OPEX)

Since the operation of a solar tower plant relies on free solar irradiance as the energy source, the running costs are notably reduced when compared with conventional fossil fuel power generation. As a result, the OPEX of a solar tower plant is small compared with the initial investment, although it still remains significant. Fig. 53 shows a typical OPEX cost breakdown for a molten salt solar tower.

Figure 53: Typical OPEX Cost breakdown for 110MW Solar Tower CSP Plant with 6 hours storage capacity [62]

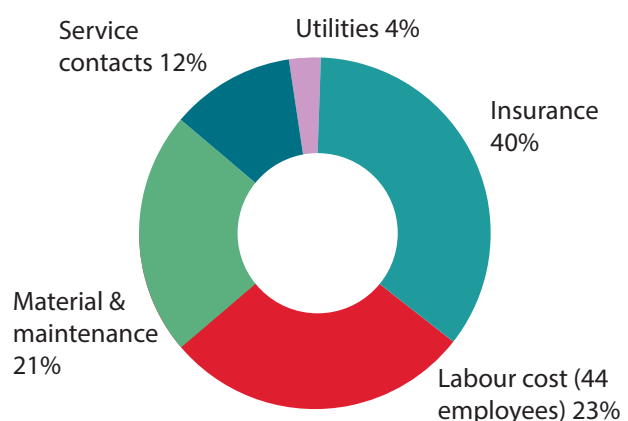The high fraction of the insurance cost is partly due to the increased risk of the new technology with limited operational experience. It is expected that the insurance cost will decrease as soon as the technology will be more mature.

6.4 REFERENCE PLANTS

As before mentioned the estimation of the real cost of a solar tower plant is not an easy task as no reliable up-to-date data are available for the few built plants. In the following three reference plants are defined, the cost breakdown as well as the LCOE are shown.

(Gross electric power) (Storage capacity at full load)	Unit	Molten salt tower Fichtner [61] 50 MW 15h TES (SM 3)	Molten salt tower Fichtner [61] 100 MW 15h TES (SM 3)	Molten salt tower CSP Today [62] 110 MW 6h TES (SM2.4)
Site information				
Site		Upington (South Africa)	Upington (South Africa)	MENA region (Algeria)
Annual DNI	kW/m²	2806	2806	2400
Mean temperature	°C	21	21	
Plant specifications				
Number of heliostats		5259	11074	10560
Heliostat reflective area	m²	121	121	112.3
Net aperture area	1000 m²	636.3	1340	1185
Solar field efficiency @DP	%	66.8	66.8	n.a.
Receiver thermal power @DP	MWth	356	713	621
Receiver aperture	m²	714	1428	-
Receiver height / diameter		17.2 / 13.2	24.3 / 18.7	20.74 / 15.56
Tower height	m	255	320	183
Storage salt mass	tons	17100	34200	16108
Steam turbine gross efficiency	%	42.1	42.1	43
Live steam condition	°C / bar	552 / 155	552 / 155	-
PB salt inlet temperature	°C	565	565	-
PB salt outlet temperature	°C	290	290	-
Plant gross efficiency @ DP	%	42.2	42.2	-
Solar to electricity efficiency @DP	%	24.4	24.4	-
Annual yields				
Gross electricity generation (total)	GWh	345	692	454.9
Own consumption (total)	GWh	30	63	39.9
Capacity factor	-	0.79	0.79	0.48
Receiver annual performance	%	85.4	85.4	-
Full load operating hours	h	6907	6923	4502 "Total operating hours"

Current Initial Investment (CAPEX)				
EPC contract costs	mln US$	501	926.7	633.9
Site preparation		19.9	42.4	41.9
Heliostat field		165.4	323.3	168.8
Receiver system		85.8	144.3	97.6
Tower		8.8	15	28.2
TES		49.3	95.3	28.5
Power block (incl. steam gen.)		65.4	110	116.1
Balance of plant		30	55	12.5
Engineering		34	62.8	89.7
Contingencies		42.5	78.5	32
Electric installation				17.4
Owners costs	mln US$	27.6	51	53.5
CAPEX grand total (+-20%)	mln US$	528.6	977.7	694.6
Specific CAPEX	US$/kW	10572	9777	6315
OPEX				
Fixed O&M costs	mln US$	9.47	16.24	8.77
Solar field & storage system		3	5.63	
Power block		1.43	2.48	
Personnel		3.06	4.5	2
Insurance		1.98	3.64	3.47
Spare parts, contract services & utilities				3.3
Variable O&M Costs	mln US$	0.89	1.78	
Total OPEX	mln US$	10.4	18.0	8.77
In percent of CAPEX	%	1.96	1.84	1.26
Levelized cost of electricity (LCOE)				
Net electricity production	GWh/a	315.5	629.6	417.1
Total CAPEX	mln US$	528.6	977.7	694.6
Total annual costs	mln US$	63.6	116.6	-
LCOE, 8% discount rate	Cent/kWh	20.2	18.5	
LCOE, 10% discount rate, 12% equity IRR, debt/equity: 70%/30%	Cent/kWh			16.2 to 18.0

7 COMPANY PROFILES

The following table displays a basic overview of the most important companies for solar tower plants. They are divided into the categories EPC contractors and component manufacturers, however both business cases are often closely connected.

EPC contractors	Main Business Area	Employees	Revenue	Solar tower track record	Owners and shareholders
Abengoa Solar www.abengoasolar.es	Concentrated solar power (parabolic through, solar tower, dish) Photovoltaics	2012: 1247 2011: 771 2010: 480 [72]	2012: 418 2011: 345 2010: 168 Million Euro [72]	Operational: PS 10, PS 20 - 30 MW Under construction: Khi Solar One – 50 MW [71]	Privately owned
BrightSource Energy www.brightsourceenergy.com	CSP Solar towers for electricity and industrial processes [73]	> 400 [73]	2012: 291 2009: 12 Million USD [74]	Operational: Coalinga, 29 MWth (steam for oil extraction) Under construction: Ivanpah, 370 MW [71]	Privately owned
eSolar www.esolar.com	Solar tower plants	50-200 [75]		Operational: Sierra sun tower, 5 MW ACME Rajasthan, 2.5 MW Under construction: Bikaner solar thermal project part 2, 7,5 MW (with ACME) [71]	Venture backed privately owned
SolarReserve www.solarreserve.com	Solar tower plants (tower)	50-200 [77]		Under construction: Crescent Dunes, 110 MW [71]	Venture backed privately owned
Aalborg CSP www.aalborgcsp.com	Steam generators for CSP plants (tower and Parabolic trough), CSP module systems, gas and oil-fired steam boilers	10-50 [78]		Operational: PS 20, 20 MW (receiver)	Privately owned
Babcock and Wilcox www.babcock.com	EPC for fossil, renewable, nuclear power and machinery Partnership with eSolar	2012: 14000 2011: 12700 [79]	2012: 3291 2011: 2952 2010: 2689 Million USD [79]	2012: 3291 2011: 2952 2010: 2689 Million USD [79]	Privately owned
Bechtel www.bechtel.com	Engineering, construction, project management in energy, transportation, communications, mining, oil, gas and government sector	2012: 53000 [80]	2012: 37900 2011: 32900 2010: 27900 2009: 30800 Million USD [80]	Operational: Solar Two, 10 MW (EPC, engineering) Under construction: Ivanpah 370 MW (EPC) [71]	Privately owned
ALSTOM www.alstom.com	Power generation, power transmission, rail infrastructure Partnership with BrightSource	2012: 94500 (9800 Renewables) 2011: 94000 (9600 Renewables) 2010: 94600 [81]	2012: 20269 2011: 19934 Million Euro [81]	Operational: Ain Beni Mathar ISCC hybrid solar-gas plant (turbomachinery) Under construction: [71]	Privately owned

8 TECHNOLOGY DEVELOPMENT PERSPECTIVE

This chapter summarizes the current R&D trends in solar tower technology. For each component, the improved technological approaches are described and their impact is discussed.

As solar tower technology is in an early stage of market deployment, a variety of technological improvements are proposed and investigated by manufacturers and research institutions. Current R&D effort for solar tower systems, with the overall goal of LCOE reduction, is focusing on the following topics:
- Cost reduction
- New technologies, resulting in lower specific investment cost
- Reduced O&M cost
- Performance improvement:
- Increased efficiency
- Advanced control strategies

The following chapters summarize the current development approaches for the different components of a solar tower system. A more detailed discussion is included in Chapter 4.

8.1 HELIOSTATS

As the heliostat field has the largest investment cost share, it offers also a high potential for future cost reduction. Kolb et al. [17] and Pfahl [10] presented a detailed discussion of different approaches and new concepts.

While some companies tend to build heliostats bigger (e.g. Abengoa: 140m² for Khi Solar One), others promote the use of very small heliostats (eSolar, Thermata) as more cost-effective. Larger heliostats offer lower specific cost for the drives (especially with hydraulic actuators), however the heliostat structure gets more costly due to the increasing wind loads. Small heliostats, installed near the ground, experience low wind loads, but the total number of drive units is very high. Currently, there is no clear indication which approach will be more cost-effective in the future. The implementation of wireless field communication is also considered to reduce field cost, eventually combined with local PV power supply to build fully autonomous heliostats that do not require any cabling.

Developments on the mirrors include sandwich structures with thin glass mirrors or reflective films attached to them. Cost reduction, quality and durability of these sandwich facets need to be verified before a wide market penetration.

The manufacturing approach has a significant impact on the cost of heliostats. Therefore, improved manufacturing technologies are developed in combination with technological advances. Improved manufacturing includes the implementation of mass production technologies (from automotive and glass industry) and components engineered for low cost (reduced complexity of parts, reduction of number of parts, use of available mass-produced parts, design with cheaper interconnection technologies like bolting). Technological advances include innovative drive concepts (e.g. hydraulic drives, rim drive) and new facet designs (e.g. sandwich facets). Manufacturing of heliostats plays also an important role in the so-called "local content", i. e. the amount of the added value that is provided by local and national resources. Compared to other renewable energy technologies, CSP offers the potential for high local content and is therefore considered by many governments as a good opportunity for job creation.

8.2 LAYOUT AND PLANT CONTROL

Layout tools will be improved to allow for more flexibility in the positioning of the heliostats, including positioning on profiled terrain and with consideration of seasonal effects. However, the improvement potential here is expected to be limited.

Advanced control methods will be implemented in the control software, enabling the plant operation to be optimized according to specific requirements. These methods can be implemented step by step into the current technology.

8.3 RECEIVER AND HEAT TRANSFER MEDIUM

A comprehensive review of innovative receiver technologies is given by Ho et al. [22]. For the current receiver technology for direct steam generation or molten salt, the development efforts are towards higher acceptable solar flux densities, resulting in smaller and cheaper receivers with higher efficiency. An efficiency increase is also expected from the development of selective absorber coatings, although the gain will be limited due to the overlapping spectra of the solar and the thermal radiation. These improvements are likely to be implemented within a few years.

In combination with advanced heat transfer media the receiver development aims at higher receiver temperatures while maintaining good thermal efficiency. The proposed advanced heat transfer media are:
- Molten salt with higher temperature stability, for temperatures up to 700°C, potentially also used as storage medium
- Liquid metals, for temperatures up to 1000°C; indirect storage system using another storage medium must be developed
- Solid particles: Also used as storage material, for temperatures up to 1000°C
- Entrained particles: Particles disappear (oxidize) when heated, for temperatures up to 1000°C and higher; regenerator-type (fixed bed) storage can be applied
- Other gases like Helium or CO_2: These gases offer improved heat transfer and will enable smaller and more efficient receivers, compared to air; regenerator-type (fixed bed) storage can be applied

While molten salt and liquid metal receivers will most probably use metallic tube technology, the particle receiver technology offers the possibility of direct absorption, thus reducing the requirements on the receiver materials. However, for all these concepts corrosion and degradation of the HTM itself and the structural components in contact with the HTM are major challenges and need to be solved before commercialization.

8.4 POWER BLOCK

Steam cycles are state-of-the-art in solar tower technology, with efficiencies limited by the maximum allowable temperature of the receiver and heat transfer medium. With new receiver designs and heat transfer media, this limit can be overcome. Then, modern sub- or supercritical steam cycles can be used, with increased efficiencies. However, as solar-specific components like heat exchangers also become more expensive, it is not clear yet if this results in an overall cost reduction.

Several other power cycles are proposed and under investigation, mainly
- Gas turbine (Brayton) cycles: These cycles offer high efficiencies and can be built in various configurations: Recuperated Brayton cycle, combined cycle (with steam turbine as bottoming cycle), with/without intercooling; required receiver temperatures are in the range of 950°C and higher. Hybridization is an important feature of gas turbine cycles, but further development of appropriate combustion systems for parallel or serial connection with the receiver needs to be made.
- Supercritical CO_2 cycle: This cycle offers high efficiency at moderately increased upper process temperatures (e. g. 700°C). The power

block can be potentially built at lower cost than a corresponding steam cycle. However, no commercial s-CO_2 power cycles are available today, and significant development effort is required until commercialization.

Generally speaking, the alternative power cycles offer high potential for cost reduction and improved system performance, but a high financial and manpower effort will be required to realize the advantages.

8.5 STORAGE

The focus of current research activities is on cost reductions. For molten salt systems, one-tank concepts with or without filler material are investigated. Movable separating walls are considered an option to ensure appropriate separation between hot and cold salt. The cost advantage results from the omission of the second tank. However the remaining tank is exposed to more challenging operating conditions with respect to local and temporal temperature changes.

For steam cycles the combination of sensible and latent heat storage is proposed to better adapt the storage characteristic to the requirements of the steam cycle. In such a system the evaporation is done within the latent heat storage part, with pre- and superheating being done in the sensible storage part.

In solid particle systems the storage is realized by simply collecting the hot particles in an insulated container. Here the challenge is more on the integration with the power cycle, as cost-effective heat exchangers (e. g. steam generators) do not exist yet.

For gases the regenerator-type storage is favored, which can be potentially cheap. Depending on the receiver and cycle configuration, large pressurized

containments must be provided, driving the cost up. Modular regenerator storage ("CellFlux") is also proposed for liquid heat transfer media, using an intermediate gas loop for heat exchange. Thus, advanced heat transfer fluids for improved receiver performance can be combined with low-cost storage solutions. However, further development must verify that the reduced storage cost overcompensates the additional cost for components and the losses by parasitics and temperature gradients in the heat exchangers.

8.6 CURRENT CSP R&D PROGRAMS

Important active R&D programs on CSP including solar tower technology are:

Research Program "Horizon2020" (EU)

Planned calls related to CSP within this program cover the following topics
- Making CSP plants more cost competitive – increasing the efficiency and reducing the construction, operation and maintenance costs of CSP plants are the main challenges. Innovative solutions and concepts are necessary in order to increase plant performance and reduce cost through improved components, improved plant control and operation, and innovative plant configurations.
- Concentrated Solar Power (CSP): Improving the environmental profile of the CSP technology – CSP plants rely on water for cleaning the reflecting surfaces, for power generation and for cooling. Innovative solutions are needed to significantly reduce or replace the water consumption while maintaining the overall efficiency of the CSP plants, and limiting their environmental impact.
- Concentrated Solar Power (CSP): Improving the flexibility and predictability of CSP generation – The major asset of the CSP technology is to be able to produce predictable power, which provides the

flexibility to adapt the demand from the grid. Only a few CSP technologies allowing this predictability have reached commercial maturity. The challenge is to demonstrate solutions that can significantly improve the dispatchability of CSP plants.

EERA Joint Programme on Concentrated Solar Power (CSP) (EU)

The overall objective of this Joint Programme is to integrate and coordinate the scientific collaboration among the leading European research institutions in CSP in order to contribute to the achievement of the targets set by the 'Solar Thermal Electricity-European Industrial Initiative (STE-EII):
- Reduction of generation, operation and maintenance costs
- Improvement of operational flexibility and energy 'dispatchability'
- Improvement in the environmental and water-use footprint
- Advanced concepts and designs

SunShot Concentrating Solar Power Research and Development (USA)

The program aims at significant improvements across all four major CSP subsystems — solar fields, power plants, receivers, and thermal storage — to achieve the SunShot cost goal of $0.06/kWh. Combined with other CSP programs focused on thermal storage improvements, the SunShot Initiative targets all major subsystems to put them on a pathway toward achieving grid parity.

Australian Concentrating Solar Power Development Programme (Australia/USA)

The Commonwealth Scientific and Industrial Research Organisation (CSIRO) is leading a program funded with AUD87 million to drive down the cost of CSP from about 25 to 10 Cts/kWh. CSIRO is partnering with six Australian universities and US'

National Renewable Energy Laboratory (NREL), Sandia National Laboratories and Arizona State University to drive the Australian Solar Thermal Research Inititative (ASTRI). Major topics are:
- Optimisation of central receivers for advanced power cycles ($3.2 million): To inform and improve modelling of optics and heat transfer through knowledge of actual heliostat and receiver performance and costs for Concentrating Solar Power systems.
- Australian Solar Energy Forecasting System ($7.6 million): Providing an accurate forecasting system to enable solar energy generation integration into the grid.
- Plug and play solar power ($2.9 million): Simplifying the integration, accelerating the deployment and lowering the cost of incorporating solar energy with more traditional non-renewable generation by developing a 'plug and play' technology.
- Deployment of combined cycle using solar reformed gas in North Western Australia ($0.7 Million): developing a renewable combined cycle power plant using solar thermal energy to upgrade abundant natural gas into synthesised gas with a higher chemical energy content.

8.7 SUMMARY

Several technological improvements are proposed and investigated in order to reduce the LCOE of solar tower systems. A detailed assessment of the potential contributions to LCOE cost reductions is presented in [67]. The possible cost reduction is shown in Fig. 54. Cost reductions are likely to occur in all components, due to technological improvements, lessons learned and mass production.

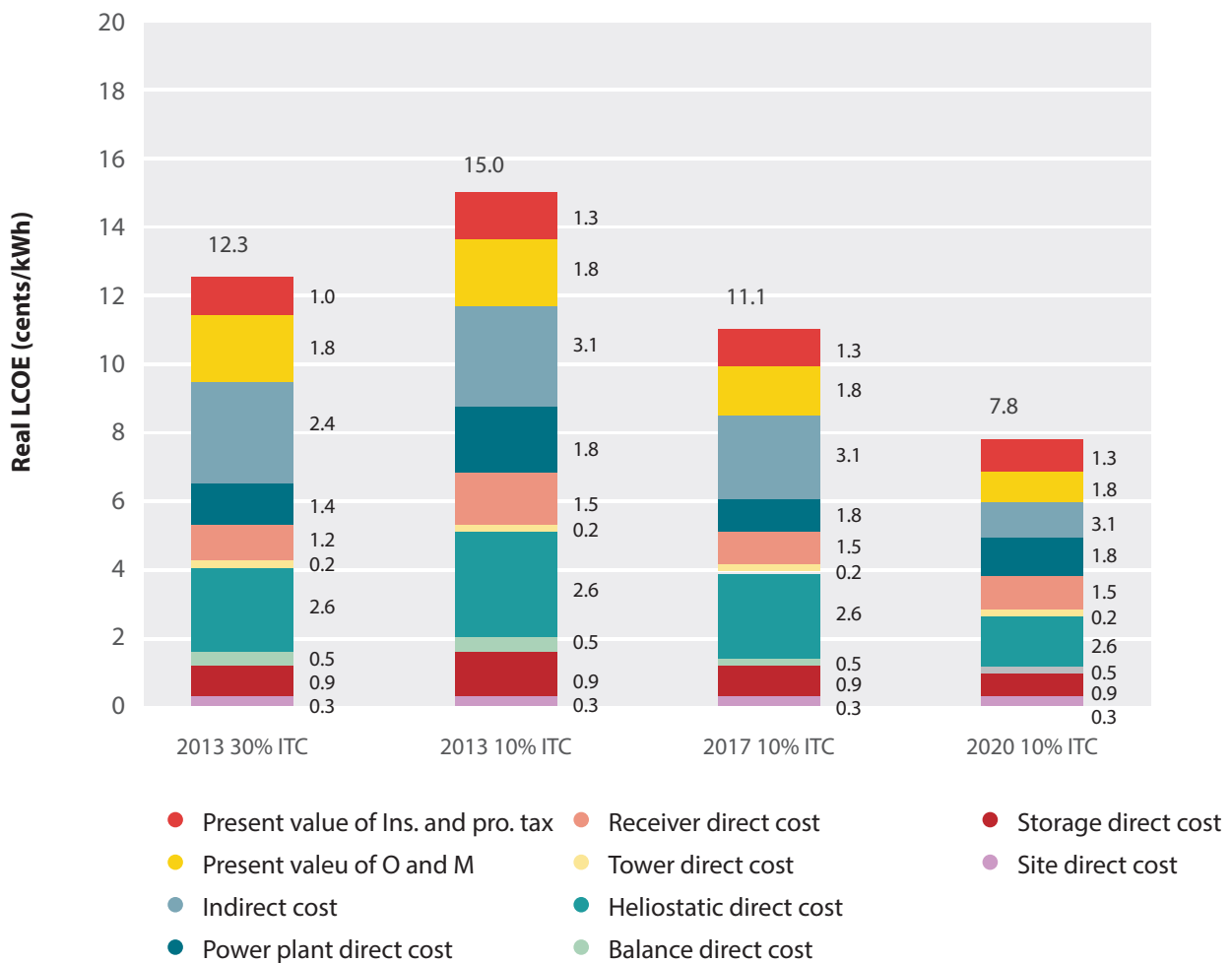Figure 54: Future cost reduction potential by contributions [67]

Technological breakthroughs are not expected to enter the market within the next 5 years. The more innovative technologies require significant further development to bring them to a Technology Readiness Level (TRL) that allows implementation in new solar tower plants. Therefore, these innovations are expected to enter the market in a longer time perspective.

9 ACRONYMS

CAPEX   capital expenses

CSP   concentrating solar power

DAR   direct absorption receiver

DNI   direct normal insolation

DP   design point

HTF   heat transfer fluid

HTM   heat transfer medium

LCOE   levelized cost of electricity

OPEX   operational expenses

O&M   operation and maintenance

PV   photovoltaic

SM   solar multiple

10 REFERENCES

http://solargis.info/doc/88

CSP Today Global Tracker, http://social.csptoday.com/tracker/projects

D. Stolten, V. Scherer (Eds.): Transition to Renewable Energy Systems, June 2013, ISBN 978-3-527-33239-7, Wiley-VCH, Weinheim (chapter 17: Solar Thermal Power Production)

Factbook Concentrating Solar Power, SBC Energy Institute, June 2013 report (available for download at: http://www.sbc.slb.com/sbcinstitute.aspx)

Hinkley, J. et al. (2011), Concentrating Solar Power-Drivers and Opportunities for Cost-competitive Electricity, CSIRO, Victoria

M. Geyer, W. Stine: http://www.powerfromthesun.net/

O. Behar, A. Khellaf, K. Mohammedi: A review of studies on central receiver solar thermal power plants, Renewable and Sustainable Energy Reviews 23 (2013) 12-39

C.-J. Winter, R. L. Sizmann, L. L. Vant-Hull: Solar Power Plants: Fundamentals, Technology, Systems, Economics

Mancini, T. R., 2000, "Catalog of Solar Heliostats," SolarPACES Technical Report No. III-1/00

Pfahl, A., 2014, "Survey of Heliostat Concepts for Cost Reduction", Journal of Solar Energy Engineering, 136 (1)

Buck, B., Pfahl, A., and Roos, T. H., 2012, "Target-Aligned Heliostat Field Layout for Non-Flat Terrain," Proceedings of 1st Southern African Solar Energy Conference, Stellenbosch, South Africa, May 21–23

Schramek, P., Tanner, A., Lievre, P., 2008, "Solar Energy Collector Heliostat", International Patent WO2008/092194A1 (but basic idea already published before)

CSIRO, 2010, "Sunny Future for Australia's Solar Industry," Science Image, accessed January 28, 2014, http://www.scienceimage.csiro.au/mediarelease/mr10-124.html

Pfahl, A., Randt, M., Holze, C., and Unterschütz, S., 2013, "Autonomous Light-Weight Heliostat With Rim Drives," Solar Energy, 92, pp 230–240

Buck, R., Wurmhöringer, K., Lehle, R., Göttsche, J., and Pfahl, A., 2010, "Development of a 30m² Heliostat With Hydraulic Drive," Proc. SolarPACES 2010 Conference, Perpignan, France, September 21–24

Holze, C., Brüggen, H., Misseeuw, R., Cosijns, B., Albers, R., Isaza, D., Buck, and R., Pfahl, A., 2012, "Laminated Solar Thin Glass Mirror Solution for Cost Effective CSP Systems," SolarPACES 2012 Conference, Marrakesh, Morocco, September 11–14

Kolb, G. J., Jones, S. A., Donnelly, M. W., Gorman, D., Thomas, R., Davenport, R., and Lumia, R., 2007, "Heliostat Cost Reduction Study," Sandia National Laboratories, Albuquerque, NM, Report No. SAND2007-3293

Kubisch, S., Randt, M., Buck, R., Pfahl, A., and Unterschütz, S., 2011, "Wireless Heliostat and Control System for Large Self-Powered Heliostat Fields," SolarPACES 2011 Conference, Granada, Spain, September 20–23

Pfahl, A., Buselmeier, M., and Zaschke, M., 2011, "Determination of Wind Loads on Heliostats," SolarPACES 2011 Conference, Granada, Spain, September 20–23

Pfahl, A., Brucks, A., Holze, C., 2013, „Wind Load Reduction for Light-Weight Heliostats", SolarPACES 2013 Conference, Las Vegas, USA, September 17-20

P. Schwarzbözl, M. Schmitz, R. Pitz-Paal, "Visual HFLCAL – a Software Tool for Layout and Optimization of Heliostat Fields". 15. International SolarPACES Symposium, Berlin, Germany (2009)

C. K. Ho, B. D. Iverson, Review of high-temperature central receiver designs for concentrating solar power, Renewable and Sustainable Energy Reviews 29 (2014) 835-846

C. K. Ho, A. R. Mahoney, A. Ambrosini, M. Bencomo, A. Hall, T. N. Lambert, Characterization of Pyromark 2500 Paint for High-Temperature Solar Receivers, J. Sol. Energy Eng. 136(1), 014502 (Jul 22, 2013)

Torresol, "Gemasolar: how it works", available for download at http://www.torresolenergy.com/EPORTAL_DOCS/GENERAL/SENERV2/DOC-cw4cb709fe34477/GEMASOLARPLANT.pdf

http://www.csp-world.com/cspworldmap/kuraymat-iscc

Stone KW, Lopez CW. Evaluation of the solar one track alignment methodology. Solar Energy 1995;1:521–6.

Kribus A., Vishnevetsky I., Yogev A., Rubinov T., Closed loop control of heliostats. Energy 29 (2004), pp. 905-913

Kistler B. L., A User's Manual for DELSOL3: A Computer Code for Calculating the Optical Performance and Optimal System Design for Solar Thermal Central Receiver Plants. SANDIA Report SAND86-8018, Albuquerque, USA, 1986

Walzel, M.D., Lipps, F.W., Vant-Hull, L.L., A solar flux density calculation for a solar tower concentrator using a two-dimensional hermite function expansion. Solar Energy 19 (3), 1977, 239–253

Lipps, F.W., Vant-Hull, L.L., 1978. A cellwise method for the optimization of large central receiver systems. Solar Energy 20, 505–516

García-Martín, F. J., Berenguel, M., Valverde, A., and Camacho, E. F., 1999, "Heuristic Knowledge-Based Heliostat Field Control for the Optimization of the Temperature Distribution in a Volumetric Receiver," Solar Energy, 66(5), pp. 355-369.

Vant-Hull, L. L., 2002, "The Role of "Allowable Flux Density" in the Design and Operation of Molten-Salt Solar Central Receivers," Journal of Solar Energy Engineering, 124(2), pp. 165-169.

Belhomme B, Pitz-Paal R, Schwarzbözl P.: Optimization of Heliostat Aim Point Selection for Central Receiver Systems Based on the Ant Colony Optimization Metaheuristic. Journal of Solar Energy Engineering 2013;136(1)

Nolteernsting F., Abel D., Göhring F.: How to maximize the output of a given power plant: Implementation of an operation assistance system in a solar power tower. SolarPACES international symposium 2013. Las Vegas, USA.

http://www.nrel.gov/csp/solarpaces/

http://www.upcomillas.es/catedras/crm/report05/Comunicaciones/Mesa%20IV/D.%20Valerio%20Fern%C3%A1ndez%20-%20Solucar%202.pdf

http://www.abengoasolar.es/web/en/galeria/

http://www.abengoasolar.es/export/sites/abengoasolar/resources/pdf/

20130502_IA_en.pdf

J. I. Burgaleta et. al., OPERATIVE ADVANTAGES OF A CENTRAL TOWER SOLAR PLANT WITH THERMAL STORAGE SYSTEM, Proc. IEA SolarPACES 2009 conference, September 15 – 18, 2009, Berlin, Germany

J. I. Burgaleta et. al., GEMASOLAR, THE FIRST TOWER THERMOSOLAR COMMERCIAL PLANT WITH MOLTEN SALT STORAGE, Proc. IEA SolarPACES 2011 conference, September 20 – 23, 2011, Granada, Spain

J. Lata et. al., COMMISSIONING AND OPERATION OF COMMERCIAL SURROUNDING HELIOSTAT FIELDS FOR MAXIMUM BUT SAFE PRODUCTION, Proc. IEA SolarPACES 2011 conference, September 20 – 23, 2011, Granada, Spain

J.M. Lata et.al: High Flux Central Receivers of Molten Salts for the New Generation of Commercial Stand-Alone Solar Power Plants, J. Solar Energy Engineering, May 2008, Vol. 130

M. Hardt, HECTOR – HELIOSTAT CLEANING TEAM-ORIENTED ROBOT, Proc. IEA SolarPACES 2011 conference, September 20 – 23, 2011, Granada, Spain

http://www.sener-power-process.com/ENERGIA/ProjectsI/gemasolar/en

P. Ricklin, C. Smith, D. Rogers, CURRENT STATUS AND FUTURE PLANS FOR ESOLAR'S SMALL HELIOSTAT BASED SOLAR COLLECTION SYSTEM, Proc. IEA SolarPACES 2011 conference, September 20 – 23, 2011, Granada, Spain

C. E. Tyner, J. E. Pacheco, eSolar's Power Plant Architecture, Proc. IEA SolarPACES 2009 conference, September 15 – 18, 2009, Berlin, Germany

G. Koll, P. Schwarzbözl, K. Hennecke, T. Hartz, M. Schmitz, B. Hoffschmidt, THE SOLAR TOWER JÜLICH – A RESEARCH AND DEMONSTRATION PLANT FOR CENTRAL RECEIVER SYSTEMS, Proc. IEA SolarPACES 2009 conference, September 15 – 18, 2009, Berlin, Germany

http://www.csp-world.com/news/20130924/001185/australias-vast-solar-gets-ok-12-mw-demonstration-csp-plant

http://aora-solar.com/

G.E. Cohen. D.W. Kearney, G.J. Kolb, Final Report on the Operation and Maintenance Improvement Program for Concentrating Solar Plants, Doc. No. SAND99-1290, (1999) Unlimited Release.

http://www.csp-world.com/cspworldmap/delingha-supcon-tower-plant

S. Zunft, M. Hänel, M. Krüger, V. Dreißigacker, F. Göhring, E. Wahl, Jülich Solar Power Tower—Experimental Evaluation of the Storage Subsystem and Performance Calculation, J. Sol. Energy Eng. 133(3), 031019 (Jul 28, 2011)

C. Winter, L. Sizman, L. Vant-Hull: Solar Power Plants, Berlin, 1991

Interatom GmbH: Technology program GAST: Gas-cooled Solar Tower Power Station, Technical Report, Bergisch-Gladbach, 1988

H. Schenk, M. Eck: Yield analysis for parabolic through solar thermal power plants - a basic approach, Technical report, enerMENA, 2012

T. Elliot, K. Chen, R.C. Swanekamp: Standard Handbook of Powerplant Engineering, Mac Graw Hill, 1997

C.S. Turchi: Supercritical CO_2 for Application in Concentrating Solar Power Systems, NREL, Proceedings of SCCO2 Power Cycle Symposium 2009, 2009

Z. Ma, C.S. Turchi: Advances Supercritical Carbon Dioxide Power Cycle Configurations for Use in Concentrating Solar Power Systems, Preprint for Supercritical CO_2 Power Cycle Symposium, NREL, Boulder, Colorado, 2011

R. Pitz-Paal, J. Dersch, B. Milow: ECOSTAR: European Concentrated Solar Thermal Road-Mapping. DLR, 2005

C. Montebello, Guidelines for the Economic Analysis of Renewable Energy Technology Applications, International Energy Agency, OECD Publications, Paris, 1991

Fichtner GmbH: Assessment of Technology Options for Development of Concentrating Solar Power in South Africa – Technical Report - Fichtner GmbH – 2010

CSP Today : CSP Solar Tower Report: Cost, Performance and Key Trends – Technical Report – CSP Today – 2012

IRENA: Renewable Energy Technologies: Cost Analysis Series, Volume 1: Power Sector, Issue 2/5, Concentrating Solar Power, June 2012

T. Mancini (ed.): Catalog of Solar Heliostats. SolarPACES Technical Report No. III – 1/00. Sandia National Laboratories, Albuquerque, USA (2000)

Romero M., Marcos M. J., Osuna R., Fernández V.: Design and Implementation Plan of a 10 MW Solar Tower Plant based on Volumetric-Air Technology in Seville (Spain). Proceedings of Solar 2000. June 16-21, 2000, Madison Wisconsin, USA

Kolb G. J., Jones S. A., Donnelly M.W., Gorman D., Thomas R., Davenport R., Lumia R.: Heliostat Cost Reduction Study, Sandia Report SAND2007- 3293, Sandia National Laboratories, 2007

G. J. Kolb, C. K. Ho, T. R. Mancini, and J. A. Gary: Power Tower Technology Roadmap and Cost Reduction Plan - SAND2011-2419, Sandia National Laboratories, 2011

http://www1.eere.energy.gov/solar/pdfs/sunshot_csp_poster.pdf

G. Weinrebe, F. von Reeken, M. Wöhrbach, T. Plaz, V. Göcke, M. Balz: Towards Holistic Power Tower System Optimization, Proc. SolarPACES 2013 Conference, Las Vegas, USA (2013)

Sargent & Lundy Consulting Group. Assessment of parabolic trough and power tower solar technology cost and performance forecasts. Report SL-5641 prepared for Department of Energy and National Renewable Energy Laboratory, 2003

CSP Today, CSP Today Global Tracker, homepage, visited 24-01-14, http://social.csptoday.com/tracker/projects

Abengoa Solar, 2012 Annual report summary, 2013

BrightSource Energy, company homepage, visited 24-01-14, http://www.brightsourceenergy.com/

Inc.com, BrightSource Energy Profile, homepage, visited 24-01-14, http://www.inc.com/profile/brightsource-energy

Linkedin.com, eSolar profile, visited 24-01-14, http://www.linkedin.com/company/esolar

SENER, SENER Annual report 2012, 2013

Linkedin.com, SolarReserve profile, homepage, visited 24-01-14, http://www.linkedin.com/company/solarreserve

Linkedin.com, Aalborg CSP profile, hompage, visited 24-1-14, http://www.linkedin.com/company/aalborg-csp-a-s

Babcock and Wilcox, 2012 Annual report, 2013

Bechtel, The Bechtel report 2012, 2013

ALSTOM, Annual financial report 2012/2013, 2013

SunShot Fact Sheet; http://www1.eere.energy.gov/solar/pdfs/55467.pdf

APPENDIX – LOCAL SUPPLY OPTIONS FOR SOLAR TOWER SYSTEMS

This appendix gives a short specification of the main components necessary for a CSP tower system. The description of specific characteristic requirements and necessary manufacturing skills should facilitate the assessment of manufacturing possibilities in Brazil.

Heliostat

Challenge: High positioning accuracy (< 1mrad), high mirror reflectivity (> 92%) over long lifetime, safe against storms, low cost

Component/part	Key raw material	Specific requirements	Skill requirements
foundation	concrete		basic technical equipment
pylon, frame	standard steel		basic technical equipment
drives (2 axes)	steel, electric motors	high precision, high durability	precise and high quality manufacturing
control	electronics, sensors	high precision, reliability	
mirrors	glass, coatings	high reflectivity and durability	glass technology
connection	cables	low cost, outdoor use	standard cable equipment

Receiver

Challenge: High efficiency, high material temperatures (600°C), long lifetime

Component/part	Key raw material	Specific requirements	Skill requirements
receiver tubes and headers	(high temperature) metal alloys	layout for long lifetime (thermal cycling, creep, ..)	plant engineering and construction
insulation	high temperature insulation material	layout for very high temperatures, shrinkage issues	experience in high temperature insulations
piping	steel, high temperature alloys	high pressure, thermal expansion compensation	plant engineering and construction
heat transfer fluid	nitrate salt, water, ..	purity of fluids	material processing, quality control

Tower

Challenge: Tower height in the range from 100 to 200m, stability under static and seismic loads, low cost, foundations important

Component/part	Key raw material	Specific requirements	Skill requirements
foundation	concrete	stability	basic technical equipment
tower	concrete or standard steel	stability under given load, high stiffness	basic technical equipment

Storage

Challenge: High temperature (560°C or higher), low cost, stability against corrosion, high storage density [kWh/m³]

Component/part	Key raw material	Specific requirements	Skill requirements
storage inventory	salt, ceramics, sand/ particles, …	high storage density, high stability against degradation	material expertise
insulation	insulation material	high temperature, low conductivity, low cost	experience in high temperature insulations
shell	(high temperature) steel	structural stability	plant engineering and construction

Power Block

Challenge: Frequent start-up/shut-down, mostly dry or hybrid cooling

Component/part	Key raw material	Specific requirements	Skill requirements
heat exchanger	steel	high temperature alloys, high steam pressure	plant engineering and construction
steam cycle	steel	plant engineering know-how	power industry
cooling	steel	plant engineering know-how	plant engineering and construction

Ministério da
**Ciência, Tecnologia
e Inovação**

GOVERNO FEDERAL
BRASIL
PÁTRIA EDUCADORA